Maghyereh and Ziadat *Financial Innovation* (2024) 10:77
https://doi.org/10.1186/s40854-023-00592-1

Financial Innovation

RESEARCH Open Access

Pattern and determinants of tail-risk transmission between cryptocurrency markets: new evidence from recent crisis episodes

Aktham Maghyereh[1*] and Salem Adel Ziadat[2,3]

*Correspondence: a.almaghaireh@uaeu.ac.ae

[1] Department of Accounting and Finance, United Arab Emirates University, Al Ain, United Arab Emirates
[2] Faculty of Business, Al-Ahliyya Amman University Jordan, Amman, Jordan
[3] Division of Accounting and Finance, University of Stirling, Stirling, UK

Abstract

The main objective of this study is to investigate tail risk connectedness among six major cryptocurrency markets and determine the extent to which investor sentiment, economic conditions, and economic uncertainty can predict tail risk interconnectedness. Combining the Conditional Autoregressive Value-at-Risk (CAViaR) model with the time-varying parameter vector autoregressive (TVP-VAR) approach shows that the transmission of tail risks among cryptocurrencies changes dynamically over time. During crises and significant events, transmission bursts and tail risks change. Based on both in- and out-of-sample forecasts, we find that the information contained in investor sentiment, economic conditions, and uncertainty includes significant predictive content about the tail risk connectedness of cryptocurrencies.

Keywords: Tail-risk connectedness, Cryptocurrency, CAViaR, TVP-VAR, Predictability

JEL Classification: C53, G1, G32, G41

Introduction

Understanding the nature and extent of the linkages among different financial markets is important for portfolio managers, investors, and policymakers. From a theoretical standpoint, (Engle et al. 1990) established heat waves and meteor shower hypotheses, wherein the heat wave refers to the notion that shocks are market-specific. Conversely, the meteor shower hypothesis suggests that shocks generated in one market are transmitted to others. Over the past few decades, the globalization of financial markets has led to higher levels of financial integration (Beine et al. 2010). Consequently, interdependence among international stock markets has grown substantially (e.g., Kim et al. 2005; Morana and Beltratti 2008). This is detrimental to international diversification and increases the transmission of shocks among financial markets (Karolyi and Stulz 1996).

Recognizing this, renewed interest in alternative asset classes such as cryptocurrencies has emerged. Indeed, cryptos are enjoying rising popularity, global reliance, and increasing trading volume. Cryptocurrencies emerged after the subprime crisis of 2008, when credit in the global financial system collapsed (Maghyereh and Abdoh 2022a; Maghyereh and Al-Shboul 2023). Constituting an attractive asset class, cryptocurrencies are often

Table 1 The sample cryptocurrencies by market capitalization

	Short name	Symbol	Total Market Capitalization	
			US$	Market Share (%)
Bitcoin	BTC		367.112 B	40.07%
Ethereum	ETC		157.149 B	17.15%
Tether	USD		68.438 B	7.47%
Binance	BNB		21.629 B	2.36%
XRP	XRP		23.765 B	2.59%
Cardano	ADA		12.524 B	1.37%
Total Market			916.070 B	71.02%

The data is based on October 15, 2022. The table depicts the market capitalization of the six chosen cryptocurrencies accounting for 71.02% of the total market capitalization. The data are obtained from https://coinmarketcap.com/

considered "safe haven" assets against other asset classes (Urquhart and Zhang 2019). First released by Nakamoto (2008), Bitcoin has received considerable attention from the media and investors. Starting humbly at 0.0001 USD in 2008, cryptocurrencies grew significantly, reaching a market capitalization of $916.070 billion in October 2022 (see Table 1). Karim et al. (2022) maintain that the growth in cryptos over the last two decades can be attributed to nonfungible tokens, decentralized financial instruments, and metaverses.

Tail risk transmission among cryptocurrencies can occur through various channels, such as market sentiment, direct investments in multiple cryptocurrencies, or spillovers from economic conditions. Several studies show a high degree of correlation among the returns of various cryptocurrencies, suggesting that tail risk transmission may be a significant issue in the cryptocurrency market. Accordingly, this study examines tail dependence between major cryptocurrencies and disentangles the underlying causes of tail dependence. The analysis incorporates Bitcoin, Ethereum, Tether, Binance, XRP, and Cardano, which constitute the six major cryptocurrencies in the market today and jointly account for approximately 71% of the overall market capitalization of cryptocurrencies.

A related subject to the financial spillover literature[1] is the hypothesis of financial contagion; the fundamental view of contagion explains the propagation of shocks across countries via real channels such as bilateral trade, trade of similar goods with a common market, monetary policy coordination, and macroeconomic similarities (see Corsetti et al. 2005). Alternatively, Forbes and Rigobon (2002) defined financial contagion as a significant increase in correlations after a shock to a single market. In other words, contagion exists if markets show a significant increase in co-movement during a crisis compared to periods of stability. This phenomenon can be explained by banking sector inefficiencies or investor herding. The 2008 subprime crisis revealed how the interaction

[1] Given that we argue for the possibility of predictability for cryptos, cryptocurrency market inefficiency is plausible and can be triggered by information asymmetries, transaction costs, and investor sentiments. Within this stream of literature, using a generalized least squares-based time-varying autoregressive model that is robust to sample size, Noda (2021) shows that the market efficiency of Bitcoin and Ethereum is time-varying and depends on volume and market capitalization. Expanding on this, Tran and Leirvik (2020) test market efficiency for Bitcoin, Ethereum, Ripple, Litecoin, and EOS. Similar to Noda (2021), the researchers argue for a time-varying composition that governs the market efficiency of cryptos. For more details, see Noda (2016) and Tran and Leirvik (2019).

between financial institutions could pose a systemic risk to the entire financial system and threaten the functioning of the financial market. Consequently, financial contagions and extreme-risk spillovers have received widespread academic attention. Consequently, multiple frameworks have been proposed to examine the risk propagation mechanisms. For example, (Diebold and Yilmaz 2009, 2012, 2014) devised the connectedness index and network topologies. Another approach involves quantile regression and CAViaR (Koenker and Hallock 2001; Engle and Manganelli 2004a; White et al. 2015), which describe the dependence structure in the median along the tail of the conditional distribution.

As financial assets, cryptocurrencies are secluded from conventional financial systems that use blockchain[2] technology (Yermack 2017). While many different variants of cryptocurrencies are available, Bitcoin was the first, created in 2009 using a scheme proposed by Nakamoto (2008), enjoying considerable market capitalization and trading volume. Using a platform similar to that adopted by Bitcoin, Litecoin is a peer-to-peer cryptocurrency introduced in 2011. Using the blockchain generated by Ethereum, Ether is a cryptocurrency that dates back to 2013. Ripple is based on the Ripple Platform, a settlement scheme introduced in 2012 (Borri 2019).

Within the literature[3] examining interrelationships among cryptocurrencies, Corbet et al. (2018) argue that Bitcoin, Litecoin, and Ripple are highly interconnected with parallel trends in returns and volatility. From a methodological standpoint, Bouri et al. (2017b), Canh et al. (2019), Katsiampa et al. (2019), and Bouri et al. (2021a, b) studied the risks of volatility connectedness among cryptocurrencies using GARCH-type models. Katsiampa (2017) compares the performance of different GARCH models in examining the links among cryptocurrencies and finds that AR-CGARCH best fits the data. While a few studies employ the wavelet coherency approach (see Omane-Adjepong and Alagidede 2019; Kumar and Anandarao 2019), a major strand of the literature exploits variants of the spillover index and network topology of variance decompositions proposed by Diebold and Yilmaz (2009, 2012, 2014) to analyze the risk spillovers among cryptocurrencies. Prominent examples include the works of Koutmos (2018), Yi et al. (2018), Ji et al. (2019), and Gillaizeau et al. (2019). Yi et al. (2018) examine multiple cryptocurrencies and find that Bitcoin is a net transmitter of volatility spillovers to other cryptocurrencies. Similarly, Ji et al. (2019) maintain that popular cryptocurrencies, such as Bitcoin, Ethereum, and Litcoin, are net transmitters of volatility. These results contradict those of Katsiampa et al. (2019), who use GARCH models to report that Bitcoin is not a dominant cryptocurrency despite enjoying the highest capitalization.

The novelty of the literature is that some studies examine the impact of exogenous variables on the connectedness of cryptos. For example, Ji et al. (2019) explored connectivity via return and volatility spillovers across six cryptocurrencies using the connectedness method of Diebold and Yilmaz (2012), Diebold and Yılmaz (2014). Their findings indicate that Litecoin and Bitcoin are at the core of an interconnected network of returns and volatility. Furthermore, their analyses reveal that trading volume, the investment substitution effect, and global financial uncertainty are the factors that determine net

[2] For a comprehensive review of blockchain literature, please refer to Xu et al. (2019).

[3] Please refer to Fang et al. (2022) for a survey of literature on cryptos trading, links, and portfolio aspects.

directional spillovers among cryptocurrencies. Sohag and Ullah (2022) used the cross-quantilogram technique to examine the impact of Twitter-based economic uncertainty on Bitcoin returns and volatility. Their findings indicated that Twitter-based economic uncertainty significantly influences volatility, whereas Bitcoin returns are net recipients. Parallel to this, Bouri et al. (2021c) expand spillover research to examine the interactions in the second moment and reveal that the entire conditional distribution of volatility connectedness is positively linked to traders' happiness at its lower quantiles of sentiment, despite the contrary being detected at the higher quantiles of investor happiness. Similarly, Al-Shboul et al. (2022) use the Quantile-VAR method to demonstrate that market uncertainty significantly impacts the interconnectedness of cryptocurrencies.

While the abovementioned studies attempt to investigate the time-varying return and volatility spillovers among cryptocurrencies, the inherent joint dynamics between extreme (tail) risks have not been directly investigated. Dynamic tail risk spillovers indicate a tail risk contagion pattern within a network of variables (Chatziantoniou et al. 2022). In this sense, analyzing tail risk connectivity is critical for examining the contagious effects among cryptocurrencies. Furthermore, previous studies used GARCH models to measure risk; however, these methods may have underestimated the structure of extreme market events (Han et al. 2016). In addition, the conditional variance characterized by GARCH models is a symmetric risk measure,[4] which makes it insufficient to examine the tail risk of a skewed distribution (Xu et al. 2021). Therefore, volatility does not accurately measure tail risk spillovers among financial assets. Additionally, the spillover index generally focuses on mean linkages and fails to account for tail dependence. Cryptocurrency returns have significantly heavier tails than traditional financial assets (Bouri et al. 2017b, a). Additionally, existing studies lack in-depth analyses of the in-sample and out-of-sample predictive power of dynamic tail risk connectedness concerning the cryptocurrency market's investor sentiment and macroeconomic and uncertainty indicators. Furthermore, some existing studies have examined the risk interconnectedness among cryptocurrencies during the COVID-19 outbreak but have not used the most updated sample period that covers the COVID-19 vaccination and Russian-Ukrainian (R-U) war.

For methodological design, we apply the conditional autoregressive Value at Risk (*CAViaR*) framework developed by Engle and Manganelli (2004a) to measure the tail risks for each selected cryptocurrency. The *CAViaR* framework uses a semiparametric approach based on autoregression to model the dynamic quantile, which, unlike the unconditional Value-at-Risk (VaR), makes no assumptions about the financial series distribution and instead explores the behavior characteristics of the distribution's tail (Engle and Manganelli 2004a). Hence, our approach is distribution-free, ideal for financial series that do not follow a normal distribution (Patton et al. 2019), and capable of capturing the volatility asymmetry and leverage effect. Subsequently, we exploit the results of the CAViaR model to explore the transmission mechanism between the tail risks of different cryptocurrencies. In detail, we use the TVP-VAR connectedness approach of Antonakakis et al. (2020) to construct the time-varying spillover among tail risks. This

[4] This runs counter to the fact that investors have a tendency to be more sensitive to the downside risk, e.g., caused by a financial crisis.

approach is advantageous as it provides information on the directions and magnitudes of connectedness in tail risks under different market conditions (i.e., during normal and crisis periods). Essentially, this method ameliorates the traditional connectedness method of Diebold and Yilmaz (2012), Diebold and Yılmaz (2014) via the following: (1) It precisely monitors parameter variations; (2) It avoids lost observations; (3) It is more robust to the existence of outliers; and (4) It does not require the selection of arbitrary window size. While several studies have investigated the tail risk of crypto-asset markets, only a few have focused on their tail-risk interconnectedness. Furthermore, to our knowledge, no study investigated the common factors that forecast the dynamic tail-risk connectedness among different crypto-asset markets. Thus, in addition to examining the extreme risk transmission between the crypto-asset markets, this study aims to investigate factors (investor sentiment, economic conditions, and economic uncertainty) that can help predict the dynamic connectedness. This is important for academics interested in joining the debate on the dynamics of contagion among cryptocurrencies. Moreover, investigating the channels behind financial contagion is important for policymakers, as they can design policies and macroeconomic strategies to mitigate contagion and preserve financial stability. Finally, the study period encompasses multiple events, including the COVID-19 pandemic and the Russian-Ukrainian conflict.

The results indicate a higher level of total tail connectedness during turbulent periods such as the COVID-19 era and the Russian-Ukrainian war. A similar trajectory of tail risk connectedness was observed at 1% and 5% risk levels. Furthermore, embedding information from the Aruoba-Diebold-Scotti Business Condition Index, Fear & Greed Crypto Index, Geopolitical Risk Index, Economic Policy Uncertainty Index, and Twitter-based Economic Uncertainty Index ameliorates the predictability of the total tail connectedness of cryptocurrencies in the system. From the perspective of pairwise connectedness, Bitcoin and Ethereum display the strongest links. Finally, despite having less capitalization than Bitcoin, Ethereum is the most influential cryptocurrency, despite the increasing dynamism of Binance, XRP, and Cardano in 2022.

The rest of the paper proceeds as follows: Section two discusses the econometric framework, while Section three details the data. Section four presents the empirical results, and section five concludes.

Methodology

Measuring tail risks

This study applies the conditional autoregressive Value at Risk (*CAViaR*) framework developed by Engle and Manganelli (2004a) to measure tail risks for each of the selected cryptocurrencies. To show tail risk explicitly, the *CAViaR* framework uses a semiparametric approach based on autoregression to model dynamic quantiles. Compared with the unconditional Value-at-Risk (VaR) method of Danielsson and Vries (2000) and *CoVaR* method of Adrian and Brunnermeier (2016), this framework makes no assumptions about financial series distribution. Instead, it explores the behavioral characteristics of the distribution's tail (Engle and Manganelli 2004). Hence, it is distribution-free and ideal for financial series that do not follow a normal distribution (Wang et al. 2018; Patton et al. 2019; Maghyereh and Yamani 2022). It can capture volatility asymmetry

and the well-known leverage effect. Following Engle and Manganelli (2004), the general *CAViaR* specifications are as follows.

$$f_t(\beta) = \beta_0 + \sum_{i=1}^{q} \beta_i f_{t-i}(\beta) + \sum_{j=1}^{r} \beta_j f_j l(x_{t-j}) \tag{1}$$

where x_t is the returns of cryptocurrency at time t, $f_t(\beta) \equiv f_t(x_{t-1}, \beta_\theta)$ is the time $t\theta-$ quantile of the distribution of cryptocurrency returns at time $t-1$, $p = q + r + 1$ is the dimension of β and $l(x_{t-j})$ is a function of a finite number of lagged values of observables (x_{t-j}). Notice that the subscript θ is omitted from β_θ in Eq. (1) for simplicity. Because of the autoregressive terms $\sum_{i=1}^{q} \beta_i f_{t-i}(\beta)$, the quantile is guaranteed to vary "smoothly" over time. The purpose of the term $l(x_{t-j})$ is to link $f_t(\beta)$ to observable variables inside the information set.

As shown by Eq. (1), VaR is affected equally by both positive and negative returns. To allow for asymmetric effects, we adopt the asymmetric slope (AS) quantile specification as follows:

$$f_t(\beta) = \beta_1 + \beta_2 f_{t-1}(\beta) + \beta_3 |y_{t-1}| I(y_{t-1} > 0) + \beta_4 |y_{t-1}| I(y_{t-1} < 0) \tag{2}$$

where y_{t-1} is the observed cryptocurrency returns at $t-1$, the coefficient β_1 is the model constant, β_2 is the coefficient on the lagged *VaR*, and the two coefficients, β_3 and β_4 capture the asymmetric (i.e., the response of *VaR* to positive and negative returns). Our analysis estimated the $AS - CAViaR$ and provided tail risks for 1% and 5% VaR levels. We used the Dynamic Quantile (DQ) test introduced by Engle and Manganelli () to ensure that the model best fits the data.

Dynamic connectedness method

In the subsequent stage, we use the results retrieved from the CAViaR model to explore the transmission mechanism between the tail risks of cryptocurrencies. This study uses the Time-Varying Parameter Vector Autoregressive (TVP-VAR) connectedness approach of Antonakakis et al. (2020) and Chatziantoniou et al. (2022) to construct a time-varying spillover among the tail risks. This approach offers a rich source of information on the directions and magnitudes of connectedness between tail risks under different market conditions (i.e., during normal and crisis periods).

Following Antonakakis et al. (2020), Chatziantoniou et al. (2022), Sohag et al. (2023a), and Cui and Maghyereh (2023a, b), we use a TVP-VAR (p) model in the following form[5]:

$$y_t = \Phi_t y_{t-1} + \epsilon_t \epsilon_t \sim N(0, S_t) \tag{3}$$

$$vec(\Phi_t) = vec(\Phi_{t-1}) + \xi_t \xi_t \sim N(0, \sqsupset_t) \tag{4}$$

where y_t is a $N \times 1$ vector of time series variables of interest (i.e., tail risk series), ϵ_t and ξ_t are an $N \times 1$ vector, Φ_t, S_t and $\sqsupset_t$ are $N \times N$ matrices. The vector autoregression with time-varying parameters, TVP-VAR(1), is then expressed by $\boldsymbol{y}_t = \sum_{i=1}^{p} \Phi \boldsymbol{y}_{t-i} + \varepsilon_t$,

[5] This section relies heavily on Antonakakis et al. (2020).

where Φ is a parameter matrix that summarizes all of the dynamic interactions among the tail risk series,[6] ε is a white noise that follows a normal distribution and $\sum$ covariance matrix. Typically, the formula for the moving average can be written as $\boldsymbol{y}_t = \sum_{i=0}^{\infty} A\varepsilon_{t-i}$.

Generalized connectedness may be determined using generalized forecast error variance decompositions (GFEVD) after the time-varying coefficients and variance–covariance matrices are computed using TVP-VAR(1).[7] Following this framework, the H-step-ahead forecast error variance decomposition is defined as

$$\theta_{ij,t}^{g}(H) = \frac{S_{jj,t}^{-1} \sum_{h=0}^{H-1} \left(e_i^{'} A_t S_t e_j\right)^2}{\sum_{j=1}^{k} \sum_{t=1}^{H-1} \left(e_i A_t S_t A_t^{'} e_i\right)}, i, j, 1, \ldots, N \tag{5}$$

where $\sum$ is the variance matrix of the vector of errors ε, and S_{jj} is the standard deviation of the error term of the *jth* variable. Finally, e_i is a selection vector with one for the *ith* element and zero otherwise. This yields an $N \times N$ matrix $\Phi(H) = \left[\Phi_{ij}(H)\right]_{ji}$, where each entry gives the contribution of variable *j* to the forecast error variance of variable *i*.

Equation (5) can be used to determine the total directional connectedness *To others* (i.e., shock variable *i* transmits its shock to all other variables *j*) as follows:

$$S_{i \to j,t}^{g}(H) = \frac{\sum_{\substack{i,j=1 \\ i \neq j}}^{N} \widetilde{\theta}_{ji,t}^{g}(H)}{\sum_{i,j-1}^{N} \widetilde{\theta}_{ji,t}^{g}(H)} \times 100 \tag{6}$$

Then, the total directional connectedness *From others* (shocks received by variable *i* from variable *j*) is calculated as

$$S_{i \leftarrow j,t}^{g}(H) = \frac{\sum_{\substack{j=1 \\ i \neq j}}^{N} \widetilde{\theta}_{ij,t}^{g}(H)}{\sum_{j=1}^{N} \widetilde{\theta}_{ij,t}^{g}(H)} \times 100 \tag{7}$$

NET total directional connectedness (i.e., the net of the influencing variable *i* to the other variables *i*) can be computed by offsetting (6) and (7) as follows:

$$S_{i,t}^{g}(H) = S_{i \to j,t}^{g}(H) - S_{i \leftarrow j,t}^{g}(H) \tag{8}$$

A positive *NET* total directional connectedness indicates that *i* variable is a net giver of shocks to another variable, whereas a negative value indicates that variable *i* is a net receiver.

Finally, the total connectivity index (TCI), which is an overall measure of how all variables are connected, can be defined as

$$S_{i}^{g}(H) = \frac{\sum_{\substack{i,j=1 \\ i \neq j}}^{N} \widetilde{\theta}_{ij,t}^{g}(H)}{N} \times 100 \tag{9}$$

[6] The Bayesian information criterion (BIC) is used to determine the optimal lag length (p = 1) in VAR.

[7] The GFEVD approach was proposed by (Koop et al. 1996) and (Pesaran and Shin 1998).

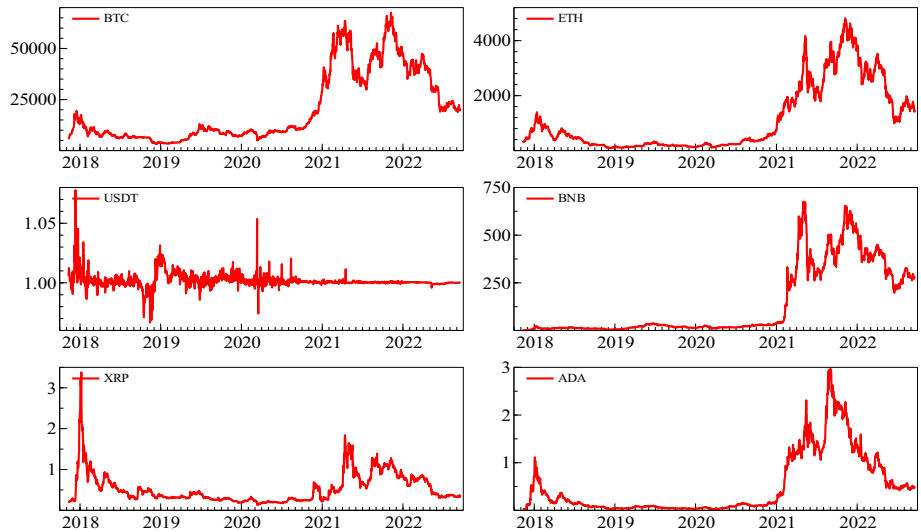

Fig. 1 Daily cryptocurrencies prices

Data

To explore the analysis, we choose Bitcoin (BTC), Ethereum (ETC), Tether (USD), Binance (BNB), XRP, and Cardano (ADA)—the six major cryptocurrencies on the market today (which together account for around 71% of the overall market capitalization of cryptocurrencies) (see Table 1).[8] The dataset contains 1786 observations of daily closing prices from September 11, 2017, to September 30, 2022.[9] The data cover the most recent crises, such as the COVID-19 pandemicpandemic and the Russian-Ukrainian conflict. The data were sourced from Thomson Reuters DataStream. For each cryptocurrency, daily continuous returns are computed as follows: $r_{it} = ln(p_{it}) - ln(p_{it-1})$, where r_{it} denotes the daily returns, and p_{it} represents the *i-th* daily price.

Figure 1 depicts the daily dynamic movements of cryptocurrency prices. The graph indicates that all cryptocurrencies have similar evolutionary patterns.[10] Prices rose abruptly in December 2018 and then fluctuated at lower levels in 2019 and 2020 before rising swiftly and reaching an all-time high in April 2021. Prices declined significantly until they began to rise again in July 2021, peaking in November 2021, and then decreasing again in March 2021.

Table 2 summarizes the descriptive statistics for the daily returns of cryptocurrencies. Binance had the greatest mean positive value, followed by Ethereum, Bitcoin, Cardano, and XRP, while Tether had a negative mean value. The tether had the lowest standard deviation, whereas the cardano had the highest volatility. All series had excess kurtosis and a heavy right tail, suggesting they were leptokurtic. The results of

[8] See https://www.statista.com/statistics/1269013/biggest-crypto-per-category-worldwide/. Furthermore, these cryptocurrencies have lately piqued the interest of investors and academic researchers (e.g., Borri 2019; Cui and Maghyereh 2022; Wang et al. 2022; Al-Shboul et al. 2022; Pace and Rao 2023; among many others).

[9] The sample's starting date is chosen on the basis of the availability of the data.

[10] Despite the high volatility and abrupt changes endured by cryptos, exploiting machine learning techniques, Sebastião and Godinho (2021) provides evidence of predictability for Bitcoin, Ethereum, and Litecoin.

Table 2 Summary statistics of daily returns

	BTC	ETC	USD	BNB	XRP	ADA
Mean	0.025	0.036	− 0.0002	0.121	0.014	0.066
Max	9.776	10.194	2.458	22.983	26.356	37.416
Min	− 20.183	− 23.918	− 2.283	− 23.585	− 23.908	− 21.872
Std. Dev	1.778	2.255	0.200	2.596	2.797	2.981
Skewness	− 0.807	− 0.910	0.693	0.385	0.832	1.925
Kurtosis	14.711	12.509	46.080	17.428	19.391	26.630
J-B	10,330.2***	6929.4***	1.373e + 5***	15,433.9***	20,065.1***	42,373.3***
ARCH (10)	3.989***	4.573***	76.455***	26.072***	14.922***	14.816***
$Q^2(20)$	59.158***	57.085***	562.959***	418.604***	295.830***	618.403***
ADF	− 23.857***	− 23.135***	− 36.939***	− 23.318***	− 23.385***	− 21.161***

BTC, Bitcoin; ETC, Ethereum; USD, Tether; BNB; Binance; XRP, XRP; ADA, Cardano. J–B is the Jarque–Bera test normality. ARCH LM is the ARCH Lagrange Multiplier test of conditional heteroskedasticity with 10 lags. $Q^2(20)$ is the Ljung-Box test of serial correlation on squared returns with 20 lags. ADF is the Augmented Dickey-Fuller unit root test. *** indicates significance at 1% level

Table 3 DQ test for CAViaR specification

	BTC	ETC	USD	BNB	XRP	ADA
Stat	6.6172	7.1777	9.4612	7.3850	8.0579	5.2530
P-value	0.3577	0.3047	0.1492	0.2867	0.2338	0.5118

BTC, Bitcoin; ETC, Ethereum; USD, Tether; BNB; Binance; XRP, XRP; ADA, Cardano. DQ is Engle and Manganelli's Dynamic Quantile test (2004) for adequacy of the estimated asymmetric slope CAViaR model. We use lagged violations lag q = 5

the Jarque–Bera test indicate that all return series are nonnormal. The ADF unit root test results reveal that all the return series are stationary.

Figure 2 shows the correlation heatmap of the six cryptocurrencies analyzed. The greater the degree of correlation, the more intense is the color (red). The graph demonstrates a strong correlation between the returns on all six cryptocurrencies. This finding is in line with those of prior studies (e.g., Hu et al. 2019; Ferreira et al. 2020; Al-Shboul et al. 2022; Cui and Maghyereh 2022; among others), which reveal that most cryptocurrency returns are positively correlated.

Empirical results

In this section, firstly, we use the model to estimate the tail risk of each cryptocurrency at the 1% and 5% levels. Second, using the TVP-VAR connectedness approach, we study the dynamic tail risk connectedness between the six cryptocurrencies, focusing on the impact of the current crises (i.e., the COVID-19 pandemic and the Russian–Ukraine conflict) on this connectivity. Finally, we perform in-sample and out-of-sample analyses to explore the role of investor sentiment and economic conditions in predicting the total connectedness of the tail risks of cryptocurrencies.

Table 4 Summary statistics of daily tail risk

	BTC	ETC	USD	BNB	XRP	ADA
Panel A: tail risk (CAViaR) at 1%						
Mean	5.032	6.589	0.401	6.718	7.912	7.307
Max	12.033	18.681	5.703	28.76	2.1737	35.721
Min	1.896	2.888	0.003	1.817	29.805	2.767
Std. Dev	2.781	4.443	0.281	14.518	22.62	15.728
Skewness	1.229***	1.644***	4.140***	2.342***	1.772***	3.349***
Kurtosis	1.729***	4.575***	28.392***	6.722***	3.205***	15.488***
J-B	667.5***	2346.4***	64,653.1***	4962.0***	1687.2***	21,047.5***
ARCH (10)	5976.8***	3099.1***	385.85***	2703.4***	3558.0***	2085.4***
$Q^2(20)$	8553.267***	7617.200***	2297.265***	7293.836***	7829.119***	6823.417***
ADF	− 2.088**	− 2.366**	− 7.136***	− 2.4106**	− 2.404**	− 2.600***
Panel B: tail risk (CAViaR) at 5%						
Mean	2.698	3.765	0.227	3.760	3.923	4.472
Max	6.51390	10.745	3.25820	16.293	14.717	22.29
Min	1.015	1.649	0.002	1.010	1.079	1.691
Std. Dev	0.804	1.457	0.09	4.561	5.555	5.935
Skewness	1.237***	1.641***	4.137***	2.341***	1.768***	3.358***
Kurtosis	1.761***	4.529***	28.301***	6.716***	3.183***	15.582***
J-B	681.9***	2311.6***	64,262.2***	4953.6***	1673.0***	21,282.1***
ARCH (10)	5394.5***	3168.7***	329.3***	2572.2***	3584.5***	1894.7***
$Q^2(20)$	8361.181***	7573.791***	2264.452***	7250.417***	7828.211***	6724.633***
ADF	− 2.093**	− 2.374**	− 7.197	− 2.402	− 2.390**	− 2.577***

This table reports the summary statistics of CAViaR at 1% and 5% using the asymmetric slope mode. BTC, Bitcoin; ETC, Ethereum; USD, Tether; BNB; Binance; XRP, XRP; ADA, Cardano. J–B is the Jarque–Bera test normality. ARCH LM is the ARCH Lagrange Multiplier test of conditional heteroskedasticity with 10 lags. $Q^2(20)$ is the Ljung-Box test of serial correlation on squared returns with 20 lags. ADF is the Augmented Dickey-Fuller unit root test. ** and *** indicate significance at 5% and 1% levels respectively

Tail risks results

Using the CAViaR model, we calculate the risk losses at 5% and 1% levels. Table 3 presents the DQ test statistics and p-values based on the adaptive specification (AS) of CAViaR for six popular cryptocurrencies. The p-values of the DQ test show that AS fits the tail risks of all cryptocurrencies. Table 4 presents the summary statistics of daily tail risk at 1% and 5% levels and shows that the risk is higher in XRP and ADA, with higher CAViaR at 1% and 5%, respectively. Figure 3 provides evidence of the substantial risks posed by XRP and ADA, especially in 2018.

Tail risks connectedness

Average connectedness

Table 5 presents the static tail risk spillovers between cryptocurrencies at 1% (Panel A) and 5% (Panel B) levels. The rows in Table 5 indicate the contribution of each cryptocurrency to the forecast error variance of a specific crypto in the system. In contrast, columns represent the effect that a specific crypto has on all other cryptos independently. In other words, the main diagonal of the matrix recaps the contribution of shocks in the market i to its own forecast error variance. The off-diagonal column sums ("To others") along with row sums ("From others") display the directional connectedness to all

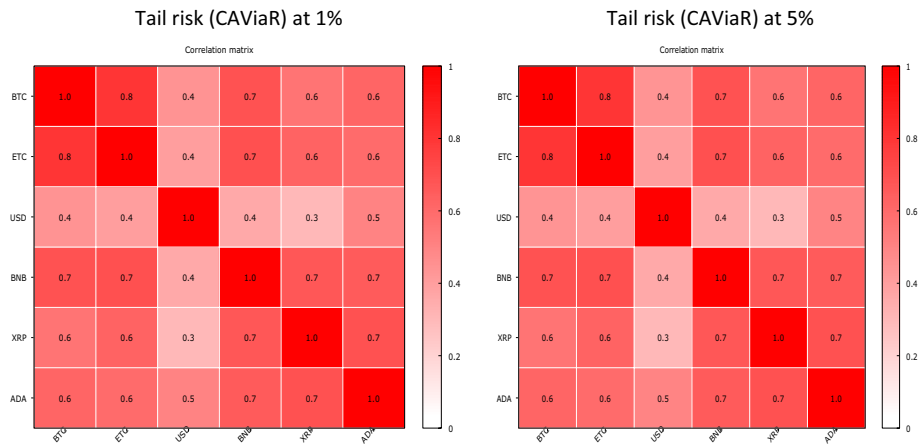

Fig. 2 Correlation heatmap matrix over the entire sample period

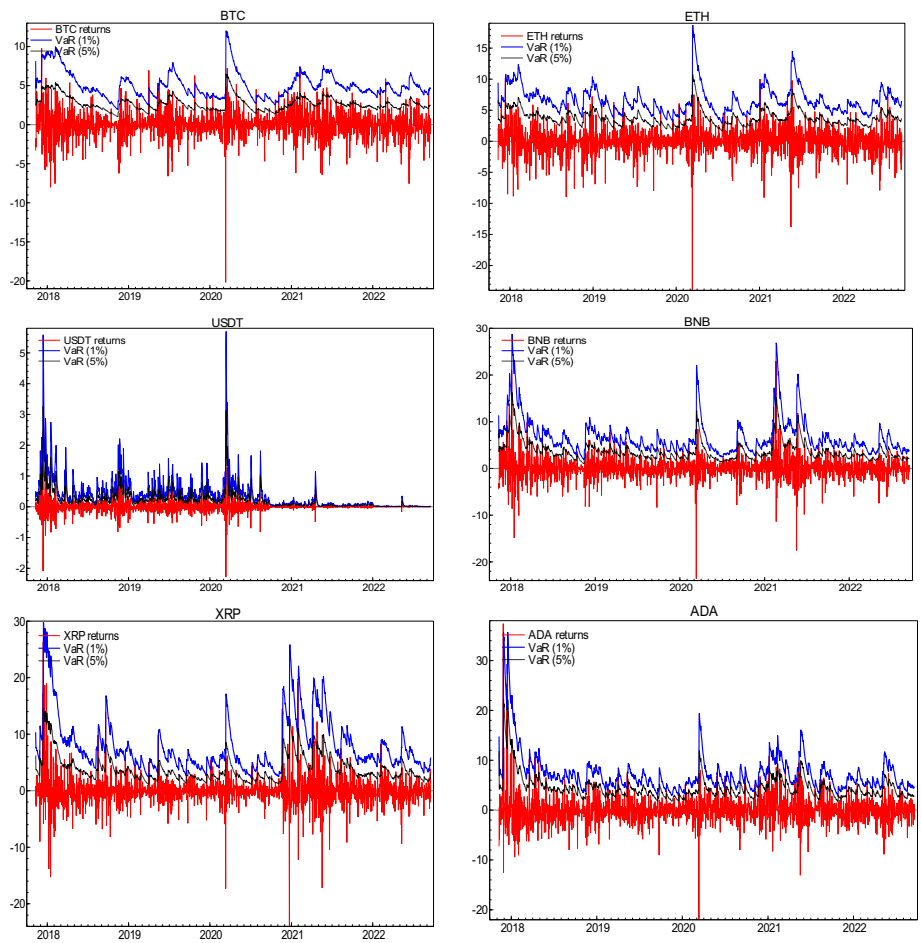

Fig. 3 Daily returns and tail risks (CAViaR) of the cryptocurrencies. *Notes*: The figure illustrates the returns and estimated 1%/5% CAViaRs of return on the six cryptocurrencies using the asymmetric slope model. The red line represents the daily returns. The blue and black lines represent VaR at 1% and 5% respectively

Table 5 Averaged connectedness among tail risks over the entire sample period

	BTC	ETC	USD	BNB	XRP	ADA	FROM others
Panel A: tail risk (CAViaR) at 1%							
BTC	**37.41**	20.57	6.01	13.72	9.93	12.37	62.59
ETC	17.62	**34.76**	4.79	15.56	13.6	13.67	65.24
USD	8.69	7.52	**66.33**	6.11	5.3	6.06	33.67
BNB	13.43	16.63	3.87	**40.41**	13.12	12.55	59.59
XRP	9.33	13.9	3.61	11.21	**48.18**	13.77	51.82
ADA	11.73	15.56	4.02	11.73	14.91	**42.05**	57.95
TO others	60.8	74.17	22.3	58.33	56.84	58.41	TCI
NET connectedness	− 1.79	8.93	− 11.38	− 1.26	5.03	0.46	66.17
NPT transmitter	1	5	0	2	4	3	
Panel B: tail risk (CAViaR) at 5%							
BTC	**38.13**	20.75	6.46	13.63	8.69	12.33	61.87
ETC	16.47	**35.52**	5.16	15.73	13.45	13.67	64.48
USD	8.59	7.47	**66.04**	6.34	5.42	6.14	33.96
BNB	12.29	16.71	4.28	**41.21**	13.16	12.36	58.79
XRP	7.53	13.65	3.87	11.12	**50.60**	13.23	49.40
ADA	11.09	15.73	4.34	11.81	14.48	**42.55**	57.45
TO others	55.98	74.31	24.1	58.63	55.19	57.73	TCI
NET connectedness	− 5.89	9.84	− 9.85	− 0.16	5.79	0.28	65.19
NPT transmitter	1	5	0	2	4	3	

The table presents the results of averaged connectedness index among tail risks (at 1% and 5% CAViaR) over the entire sample period (11/9/2017–9/18/2022) based on a TVP-VAR model with a length of order 1 selected by the BIC. The generalized forecast error variance decomposition is based on a 20-step-ahead. BTC, Bitcoin; ETC, Ethereum; USD, Tether; BNB; Binance; XRP, XRP; ADA, Cardano; TCI, total connectedness index; TO others, The transmits shock of asset i to all other assets j; FROM others, the directional connectedness asset i receives from asset j; NET connectedness, the influence of asset i, while a positive value indicates that asset i influences the network more than itself being influenced, a negative value indicates that asset i is driven by the network; NPT transmitter: net pairwise directional connectedness, A positive (negative) value indicates that asset i leads (is led by) asset j

variables in the system from i and from all others to j, correspondingly. The row "Net connectedness" represents the total sum of net-pairwise directional spillover expressed as a negative (positive) value for the net recipient (net transmitter). Finally, the TCI stands for the total connectedness index of a whole system.

Table 5 depicts the connectedness among tail risks at 1% and 5% levels. At first glance, we observed a general similarity in the results at both levels. The TCI records 65.19% at 5% and 66.17% at 1%. These observations indicate that external rather than intrinsic innovations can explain more than half of the movement forecasts. Furthermore, this result echoes the high connectedness in the tails among cryptocurrencies, which is consistent with Al-Shboul et al. (2022) findings. Indeed, at 1% and 5%, ETC, XRP, and ADA constituted net transmitters to the system, and their net pairwise directional connectedness (NPT) rankings were 1, 2, and 3, respectively. Such outcomes reflect their dominance in the network and the net pairwise setup. On the other hand, BTC, USD, and BNC are net importers of information. This result indicates that BTC lost its status as an important influencer on the movements of other cryptocurrencies, corroborating the findings of Katsiampa et al. (2019).

With readings in their 30 s for self-explained innovations, BTC and ETC are the most integrated cryptos in the system, as approximately 70% of their variances are

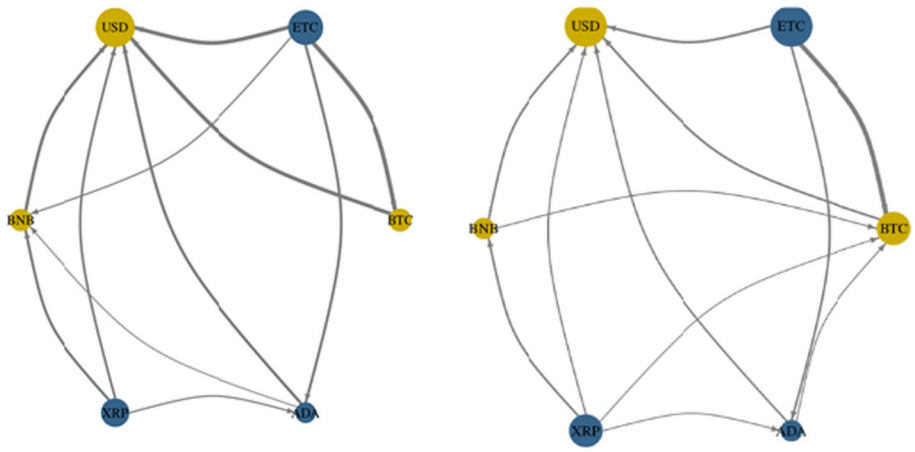

Fig. 4 Tail risk directional connectedness network over the entire sample period. *Note*: The connectedness is calculated using a TVP-VAR model with a length of order 1 chosen by the BIC. The generalized forecast error variance decomposition is based on a 20-step-ahead. Each node represents a cryptocurrency, the size of the node indicates its information contribution to the system, the width of the line denotes the magnitude of the information spillover, and the arrow symbolizes its direction

explained by external factors in the system. Parallel to that, BTC and ETC are strongly connected to each other at 1% and 5% risk levels, with around 17% of BTC variance explained by innovations from ETC and around 21% vice versa. This is in sharp contrast to USD and XRP to a lesser extent. Within the USD, approximately 66% of its forecasted innovations are self-explanatory, and external impact hovers around 33% at both 1% and 5%. These figures designate the USD as the least integrated currency in the system. Interestingly, readings such as − 11.38 at 1% and − 9.85% at 5% net connectedness values for USD make it the least influential crypto in the system.

From a directional tail risk transmission standpoint, the node size in Fig. 4 reflects the magnitude of the net sender/receiver of spillovers, which depicts the strength of the spillovers. The blue color of a node indicates that the market is a net giver of spillovers, whereas the yellow color labels it a net receiver of spillovers. Figure 4 provides information on the spillover trends regarding direction and intensity. While the results at 1% and 5% remain broadly similar, Fig. 4 presents the following discrepancies; First, at the 1% tail risk level, BNB imports information from ETC, ADA, and XRP, whereas XRP is the sole exporter of information to BNB at 5%. Second, BTC's vulnerability to innovation from ADA, XRP, and BNB evaporated at the 1% level. Such discrepancies highlight important information about the extreme spillovers and financial contagion among cryptos. Conversely, and consistent with Table 5, USD is on the receiving end of other cryptos, regardless of the risk quantile. Similarly, corroborating the findings of Xu et al. (2021), the ETC and XRP originate from important flows of tail risk innovations for other cryptos.

Time-varying connectedness

Figure 5 depicts the time-varying connectedness at 5% and 1% risk levels. Like the static model results, the tail risk connectedness follows a similar trajectory at 1% and 5% risk levels. In 2018, the connectedness index became relatively high and set around 80%

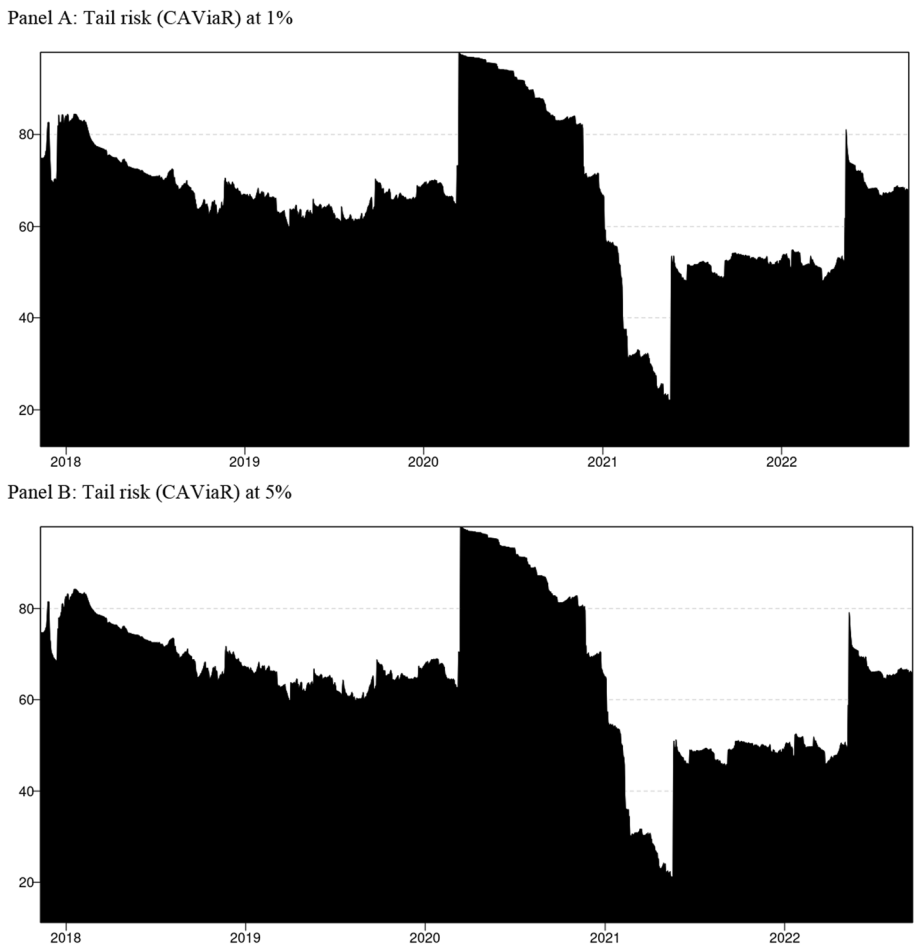

Fig. 5 Dynamic total connectedness. *Notes*: The results are based on a TVP-VAR model with a length of order 1 chosen by the BIC. The generalized forecast error variance decomposition is based on a 20-step-ahead

before increasing sharply in March 2020, reaching more than 95%. These results echo the high level of tail risk connectedness among cryptocurrencies, as Borri (2019) argues. Following Kumar et al. (2022) and Cui and Maghyereh (2022), the COVID-19 impact persisted in 2020, resulting in a soaring connectedness index throughout the year only to fall sharply in 2021; the latter can be associated with the lifting of COVID-19 precautions and "return to normal" policies. Between 2021 and 2022, the level of connectedness rebounded to a new average that hovered around 50%. However, in 2022, the TCI returned to its pre-COVID-19 average of 70% due to the geopolitical stress accompanying the Russian-Ukrainian war. The extraordinary circumstances that persisted amid the COVID-19 era and the geopolitical stress in Ukraine triggered important shifts in investor behavior, wherein higher interest in non-conventional asset classes (such as cryptos) emerged. This can be explained as follows. First, lockdowns triggered uncertainties around conventional businesses amid the COVID-19 pandemic. Second, cryptocurrencies can be an alternative means of sending transfers circumventing Western sanctions against Russia. Finally, cheap energy prices in Russia might prompt higher crypto-mining activities, especially during geopolitical turbulence and uncertain business environments.

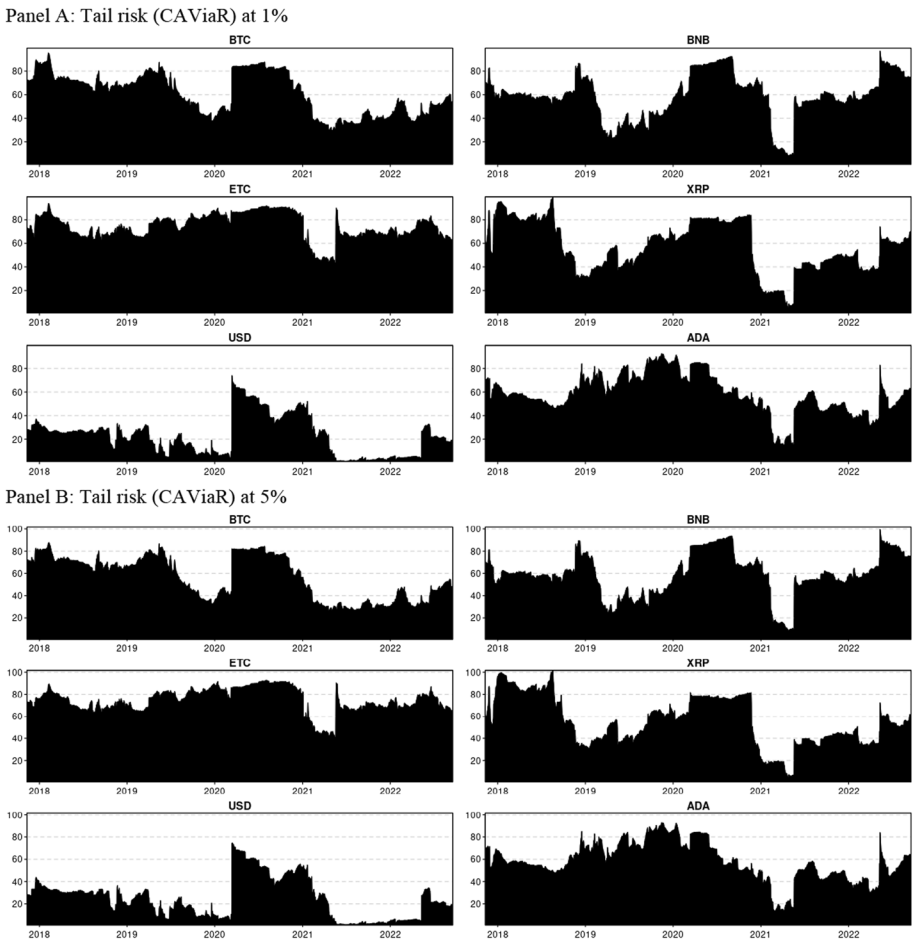

Fig. 6 Transmits shock of tail risk from asset i to all other assets. *Notes*: The results are based on a TVP-VAR model with a length of order 1 chosen by the BIC. The generalized forecast error variance decomposition is based on a 20-step-ahead

These results corroborate the findings of Gillaizeau et al. (2019), who argue that bitcoin prices display strong volatility spillovers from conventional currencies during periods of high uncertainty. Simultaneously, our results display conventional cyclical movements in risk spillovers, which contradict the increasing trend in risk connectedness proposed by Xu et al. (2021). Extreme connectedness amid turbulent circumstances may signal herding behavior among cryptocurrency traders, as (Kumar and Anandarao 2019) argued. Lastly, the total risk connectedness during the COVID-19 phase was more intense than during the Russian-Ukrainian War because of the larger scope of the former.

Figure 6 illustrates the transmission of shocks from a specific cryptocurrency to others, and Fig. 7 illustrates the transmission from other cryptocurrencies to a specific currency. Intuitively, the individual charts in Fig. 5 present the total dynamic connectedness of the system. Within this, we can see that the overall connectedness (Fig. 5) mimics the ETC chart, further reflecting ETC's large footprint in the system. This is consistent with the findings of Ji et al. (2019). While this is visible from 2018 to 2022, the increasing dynamism of BNB, XRP, and ADA can explain the higher overall connectedness in 2022. Notably, a sudden interest in specific cryptos can be linked to the "fear of missing out"

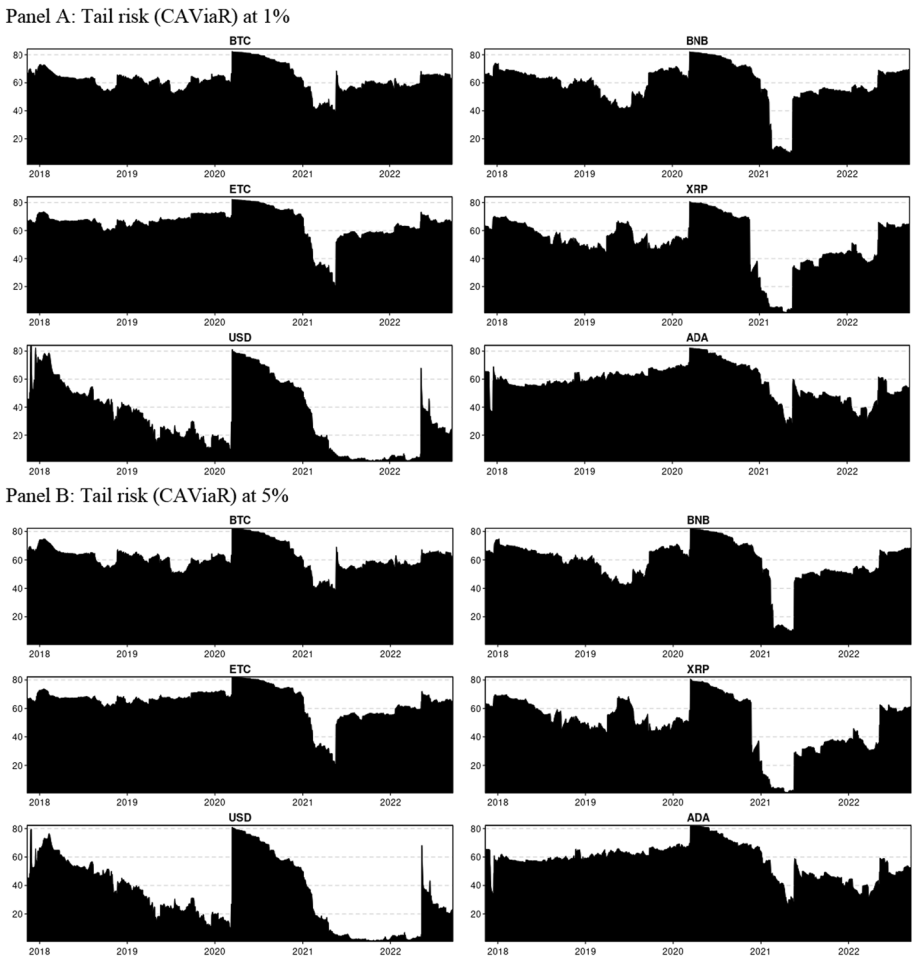

Fig. 7 The directional connectedness of one asset receives from other assets. *Notes*: The results are based on a TVP-VAR model with a length of order 1 chosen by the BIC. The generalized forecast error variance decomposition is based on a 20-step-ahead

of individual investors and may yield to financial bubbles (see Geuder et al. 2019). Essentially, our results align with those of Luu Duc Huynh (2019), who exploited Granger causality methods alongside copulas and reported that BTC tends to be influenced by ETC and XRP. However, contrary to our results, Luu Duc Huynh (2019) finds that the ETC trajectory is independent of other cryptos.

Subtracting the values presented in Fig. 7 from those in Fig. 6 produces Fig. 8, which illustrates net total directional connectedness. Mirroring the findings in Table 5, the results do not vary much at the 1% and 5% levels. ETC is the system's most dominant crypto and net contributor throughout most of the sample period. However, while being a consistent net contributor of information before 2020, BTC lost its status and became a net receiver of shocks from 2021 until the end of the sample. This outcome contradicts the results of Omane-Adjepong and Alagidede (2019) and Koutmos (2018), who argue that BTC played a dominant role in influencing other cryptos. The difference in results can be attributed to the newer sample in our study, the different econometric approach, and the high dynamism in cryptocurrency markets. The USD is the polar opposite of the

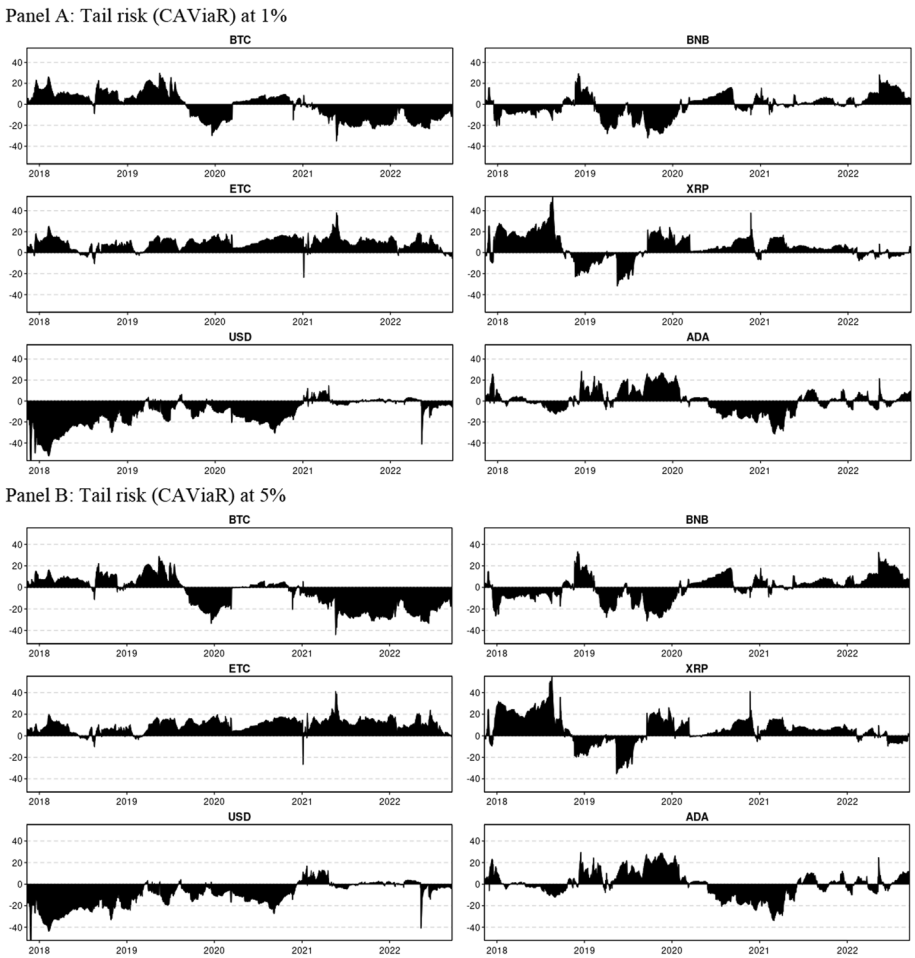

Fig. 8 Net total directional connectedness. *Notes*: The results are based on a TVP-VAR model with a length of order 1 chosen by the BIC. The generalized forecast error variance decomposition is based on a 20-step-ahead

ETC and has been a net receiver of shocks throughout most of the sample period. Likewise, the BNB acted as a net importer of shocks from 2018 to 2020 and subsequently switched to a net exporter. Finally, although both XRP and ADA fluctuate between net contributors and receivers of information, the former is generally more influential in the system.

Figure 9 shows net directional connectedness. Viewing both Panels A (depicting the tail risk at 1%) and Panel B (depicting the tail risk at 5%), we can see clear evidence of BTC losing its influence on other currencies as time passes. This can be observed in the BTC-ETC and BTC-BNB pairs. USD, whereas generally on the receiving end, received strong spills in early 2022 from the BNB, XRP, and ADA. Our results conform with those of Xu et al. (2021), who examine tail risk spillovers and report an active role for ETC and a passive role for BTC.

Figure 10 illustrates the dynamic pairwise connectedness of the sampled cryptocurrencies in an amalgamated manner. Notably, the connectedness between BTC and ETC is consistently higher than that of the other pairs, regardless of the tail risk specification and period. Both well-established and highly capitalized currencies can explain such

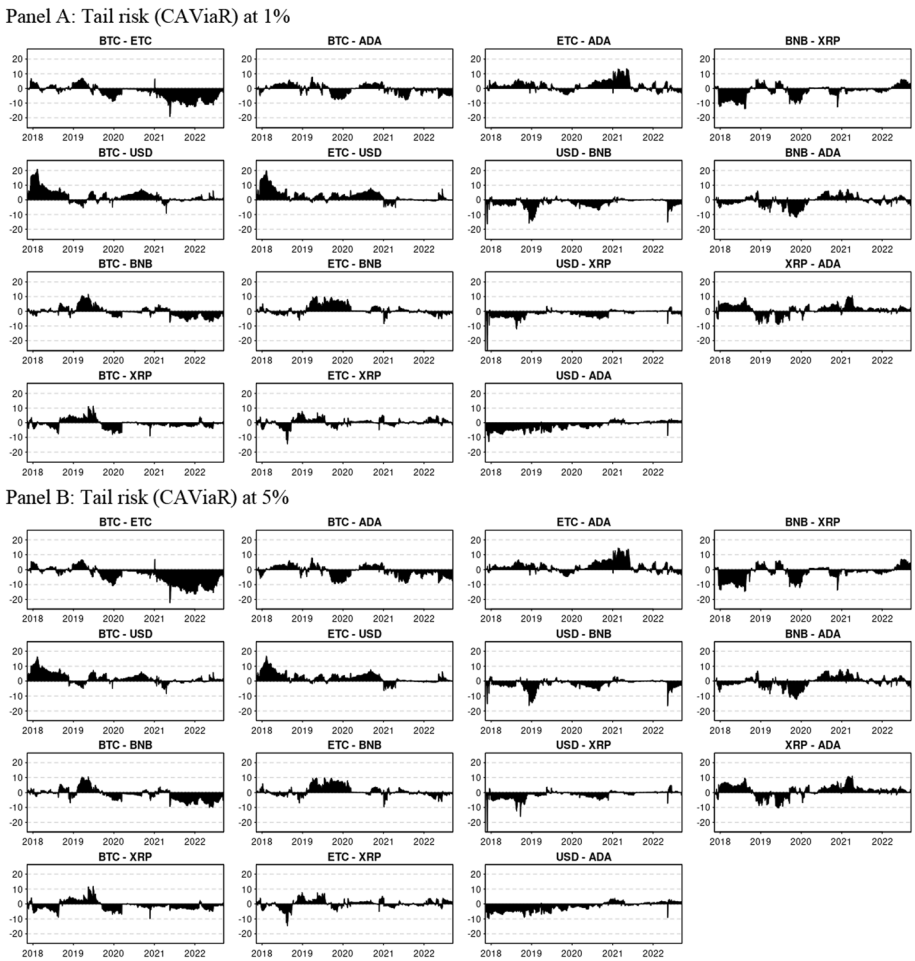

Fig. 9 Net pairwise directional connectedness. *Notes*: The results are based on a TVP-VAR model with a length of order 1 chosen by the BIC. The generalized forecast error variance decomposition is based on a 20-step-ahead

links (see Table 1). The USD and BTC pairwise connectedness with other currencies experienced a jump between 2020 and 2021, whereas a slump in 2021 occurred in the XRP and BNB connectedness with other cryptos.

The impact of investor sentiment and economic conditions on tail risks connectedness

The empirical evidence in the previous section shows that the transmission of the total tail risk among cryptocurrencies changes dynamically over time. Transmission bursts and tail risks change during crises and other significant events. Hence, we hypothesize that investor mood and economic conditions can explain tail risk transmission. We hypothesize that the transmission of tail risks may increase when fear-induced emotions increase and economic circumstances deteriorate. Therefore, this section examines the extent to which investor mood, economic conditions, and economic uncertainty can predict the connectedness among cryptocurrency tail risks.

To proxy for investor emotions and sentiment, we use the Fear & Greed Crypto Index (FGCI). This index gauges investors' behavior and emotions in the cryptocurrency

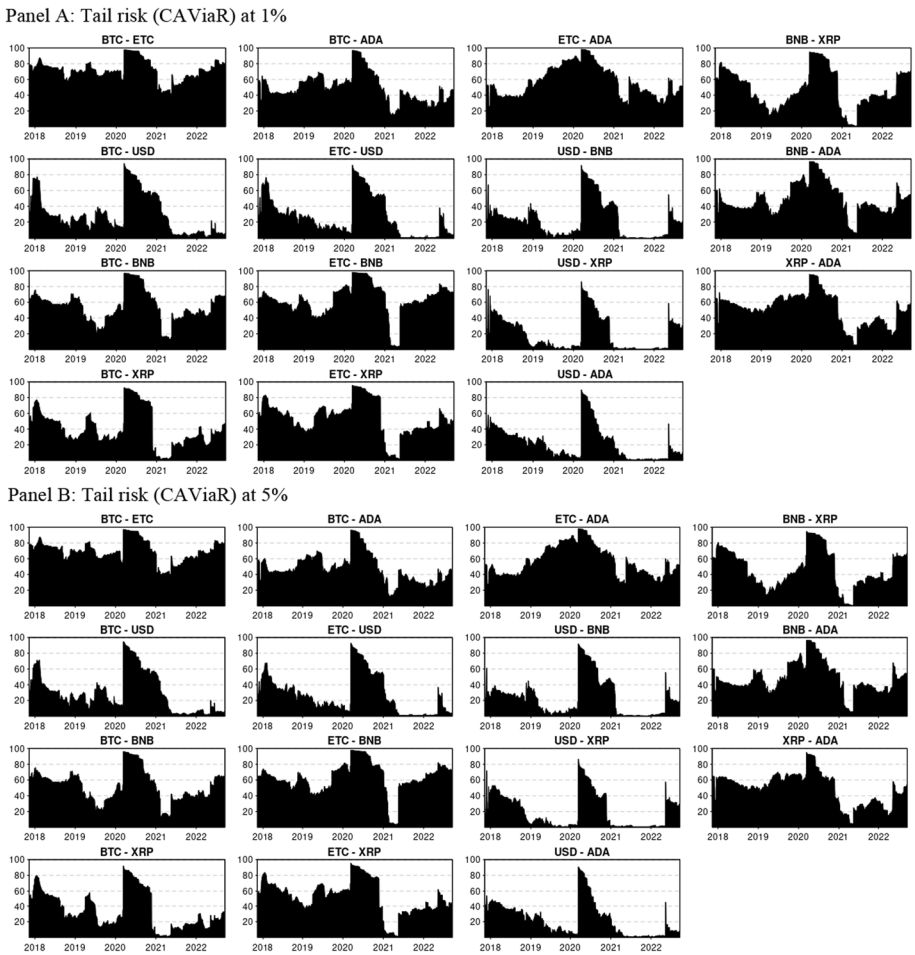

Fig. 10 Dynamic pairwise connectedness. *Notes*: The results are based on a TVP-VAR model with a length of order 1 chosen by the BIC. The generalized forecast error variance decomposition is based on a 20-step-ahead.

market. Using a needle that moves from left to right and ranges between 0 and 100, FGCI indicates whether investors are now feeling bold or afraid. The lower value represents "more fearful investors," whereas the higher value represents "more greedy investors." The value of the index is based on several factors, including the level of volatility in the cryptocurrency market, the volume of trade, social media momentum, and the dominance of Bitcoin. The FGCI data were derived from https://alternative.me/crypto/.

To proxy for economic conditions, we use the Aruoba-Diebold-Scotti Business Condition Index (ADS Index), which tracks real business conditions at a high frequency and is based on economic indicators collected at varying frequencies. An index is constructed such that its average value is zero. Progressive positive values of the index indicate progressive improvement in business conditions and a better-than-average business environment. The ADS index data were downloaded from the official website of the Federal Reserve Bank of Philadelphia at https://www.philadelphiafed.org/surveys-and-data/real-time-data-research/ads.

As uncertainty proxies, we use the Geopolitical Risk Index (the GPR index hereinafter) by Caldara and Iacoviello (2022), the Economic Policy Uncertainty Index

Table 6 Summary statistics for variables used in prediction regressions

	TCI (1%)	TCI (5%)	FGCI	ADS	GPR	EPU	TEU
Mean	65.520	65.189	43.007	− 0.313	99.483	158.464	154.084
Max	98.024	97.92	95.000	8.989	539.583	861.100	1134.894
Min	22.033	21.178	5.000	− 26.332	3.570	4.050	8.883
Std. Dev	15.268	15.849	22.679	4.153	60.922	118.927	126.612
Skewness	− 0.175	− 0.264	0.540	− 4.093	2.327	2.136	2.814
Kurtosis	3.559	2.232	2.283	25.040	12.603	8.479	13.805
J-B	30.6***	24.631***	118.4***	38,946.7***	8024.6***	3400.5***	10,458.6***
ADF	− 2.787**	− 2.060**	− 4.741***	− 4.647***	− 3.706***	− 2.801**	− 3.646***

TCI, total connectedness index; FGCI, Fear & Greed Crypto Index; ADS, Aruoba-Diebold-Scotti business condition index; GPR, geopolitical risk index; EPU, economic policy uncertainty, index; TEU, Twitter-based economic uncertainty index. J-B is the Jarque–Bera test normality. ADF is the Augmented Dickey-Fuller unit root test. *** indicates significance at 1% level

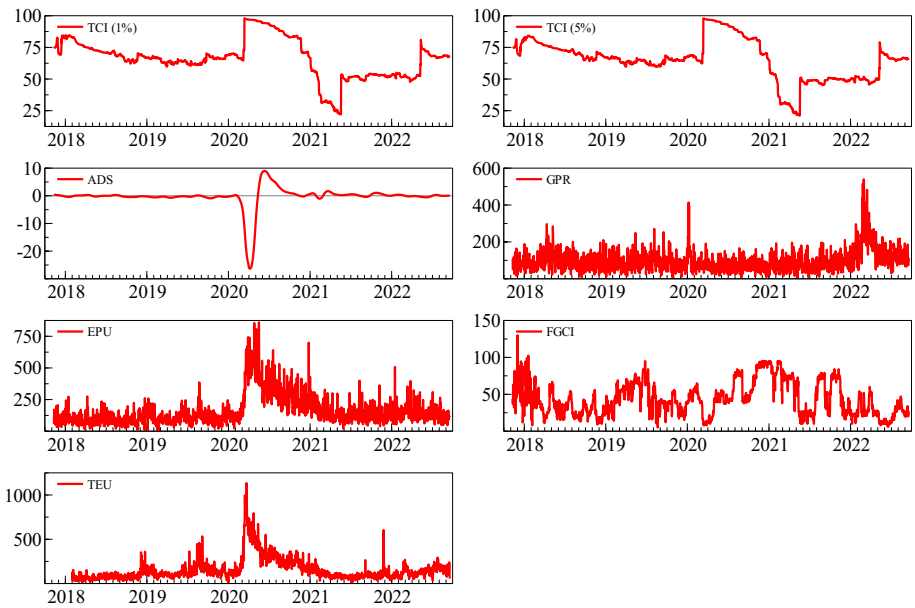

Fig. 11 Time-series plots of the variables used in the prediction model. *Notes*: TCI: total connectedness index:FGCI: Fear & Greed Crypto Index; ADS: Aruoba-Diebold-Scotti Business Condition Index; GPR: Geopolitical Risk index; EPU: Economic Policy Uncertainty; index; TEU: Twitter-based economic uncertainty index

(the EPU index hereinafter) by Baker et al. (2016), and the Twitter-based Economic Uncertainty Index (the TEU index hereinafter). Based on ten newspapers, the GPR index assesses the proportion of total news stories addressing geopolitical tensions. GPR index data were obtained from https://www.matteoiacoviello.com/gpr.htm. The EPU index measures economic policy uncertainty, and its value depends on the number of EPU articles published, the number of federal tax codes set to expire, and the number of disagreements among forecasters about future economic conditions. The TEU index is constructed based on all messages transmitted over the Twitter social media network containing keywords related to "uncertainty" and "economy." Data on

the EPU and TEU indices were downloaded from the Economic Policy Uncertainty website at https://www.policyuncertainty.com/index.html.

Table 6 presents the summary statistics for the variables used in the prediction models, and Fig. 11 depicts the daily time series of these variables. The figure shows that the ADS, while generally hovering around zero, sharply decreased around the onset of the COVID-19 pandemic. This observation mirrors the lockdown and associated business closures. On the other hand, GPR experienced more fluctuations that culminated in a peak during the Russian-Ukrainian war. TEU and EPU display similar trajectories, wherein a break was noticed between the pre- and post-COVID-19 eras in 2020. Finally, the FGCI appeared to follow a distinctive pattern away from geopolitical and biological hazards.

Causality test

Before discussing the prediction models, we check the causality between each investor mood, economic condition, economic uncertainty variable, and the connectedness of the cryptocurrencies' tail risks. For this purpose, we utilized the novel time-varying Granger causality test proposed by Shi et al. (2020). Compared with traditional Granger causality test statistics, this test is robust to heteroskedasticity, deterministic trends, and nonlinearity. Furthermore, the test is not sensitive to outliers, skewness, or time window selection (Maghyereha et al. 2022).

Table 7 reports the Wald test statistics for the Granger causality test using recursive evolving heteroskedasticity algorithms. We find evidence of Granger causality from all predictable variables to the connectedness of the cryptocurrencies' tail risks over the entire sample period. Figure 12 depicts the recursively evolving Granger causality test statistic (Wald statistic sequence) and their bootstrapped 10% and 5% critical values (lower- and upper-horizontal lines). The minimum window size is set at 60 days (two months). BIC selects the lag length for the whole sample period with a maximum lag order of 12. In graphs, if the Wald statistic sequence surpasses its corresponding critical value during a period, then a significant causality is evident. Confirming the results in Table 7, causality is evident at the 1% and 5% risk levels. Yet, a time-varying element is detected; within this, the causality running from EPU, GPR, and FGCI is short-lived, whereas ADS and TEU display a consistent causal footprint on the TCI of cryptos starting from 2020 until the end of the sample.

In-sample regression

Our analysis in this subsection is based on the following predictive model (Westerlund and Narayan 2012, 2015; Salisu et al. 2022, 2023):

$$\mathrm{TCI}_t = \beta_0 + \sum_{i=1}^{7} \beta_i X_{jt-i} + \gamma \left(X_{jt} - \varphi X_{jt-1} \right) + \varepsilon_t \tag{10}$$

where TCI_t is the total connectivity index between the tail risks of cryptocurrency at time t, X is one of the investor sentiment, economic conditions, and economic uncertainty indicators (i.e., FGCI, ADS, GPR, EPU, and TEU). We add the lags of the indicators to control for persistence. β_0 is the intercept, β_i is the coefficient of the effect of the indicator, and the error term ε is assumed to be independent and identically distributed with mean 0 and constant variance. Following Westerlund and Narayan (2012, 2015) and

Table 7 Wald test statistics for time-varying Granger causality

	Wald statistics-recursive evolving-heteroskedasticity
Panel A: tail risk (CAViaR) at 1%	
H0: TCI (1%) is Granger causality FGCI	32.871***
	− 7.023
	[10.047]
H0: TCI (1%) is Granger causality ADS	49.018***
	− 8.026
	[10.046]
H0: TCI (1%) is Granger causality GPR	21.921***
	− 6.39
	[9.543]
H0: TCI (1%) is Granger causality EPU	28.910***
	− 7.149
	[9.940]
H0: TCI (1%) is Granger causality TEU	32.791***
	− 7.098
	[9.114]
Panel B: tail risk (CAViaR) at 5%	
H0: TCI (5%) is Granger causality FGCI	26.924***
	− 6.752
	[8.731]
H0: TCI (%%) is Granger causality ADS	48.819***
	− 7.776
	[10.090]
H0: TCI (5%) is Granger causality GPR	27.582***
	− 7.389
	[9.278]
H0: TCI (5%) is Granger causality EPU	30.200***
	− 6.699
	[8.663]
H0: TCI (5%) is Granger causality TEU	33.201***
	− 6.318
	[8.619]

Wald test statistics computed using recursive evolving-heteroskedasticity algorithms. We follow Shi et al. (2020) and set the minimum window size to 72 observations. The empirical distribution of the bootstrap test statistics at the 95th and 99th percentile are shown in parentheses and brackets, respectively. *, ** and *** indicate significance at 10%, 5% and 1% levels respectively

Salisu et al. (2022, 2023), we added the term $\gamma\left(X_{jt} - \varphi X_{jt-1}\right)$ to the model to eliminate the potential endogeneity bias (that would be present due to model misspecification and/or omitted variables and structural break) as well as any potential persistence effect. Based on the aforementioned model's in-sample estimate, we examine the null hypothesis of no predictability by testing the restriction $\sum_{i=1}^{7} \beta_i = 0$ using the Wald joint test.[11] The rejection of the null hypothesis implies the predictability of the variable of interest for the cryptocurrencies' tail risk connectedness.

[11] We use a bootstrapping method to estimate our standard errors in the in-sample analysis.

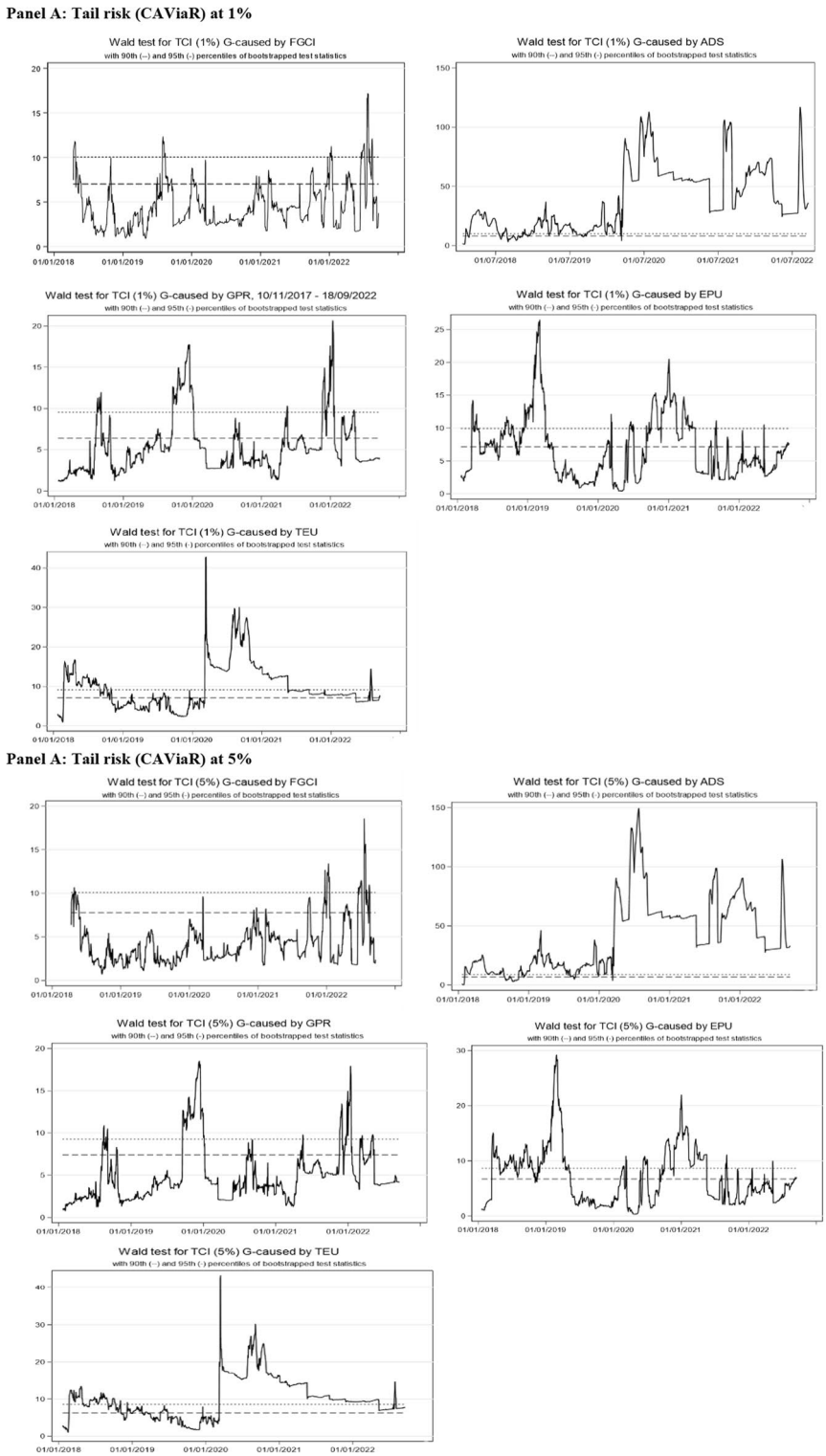

Fig. 12 Time-varying Granger causality tests. *Notes*: The time-varying causality is obtained from a lag-augmented VAR (LA-VAR) model with d = 1. The ag orders are determined by BIC. Wald test statistics computed using recursive evolving-heteroskedasticity algorithms. Like Shi et al. (2020), the 10% and 5% bootstrapped critical values (lower- and upper-horizontal lines) are based on 199 replications

Table 8 In-sample prediction

	Predictor				
	FGCI	**ADS**	**GPR**	**EPU**	**TEU**
Panel A: tail risk (CAViaR) at 1%					
Wald statistics	0.4628***	0.9825***	-0.0745***	0.0833***	0.1400***
	(0.0027)	(0.0164)	(0.0014)	(0.0008)	(0.0045)
Panel B: tail risk (CAViaR) at 5%					
Wald statistics	0.5086***	0.3966***	0.0863***	0.0618***	0.1221***
	(0.0027)	(0.0168)	(0.0015)	(0.0081)	(0.0031)

Wald statistics testing the null hypothesis of predictability that $\sum_{i=1}^{7} \beta_i = 0$. A rejection of the null hypothesis implies the predictability of the independent variables for tail-risk interdependence. Values in parentheses represent standard errors. *, ** and *** indicate significance at 10%, 5% and 1% levels respectively

Table 8 presents the results of the in-sample predictability. This table reports the Wald test statistic and the corresponding p-value for the null hypothesis, which states that the slope coefficient in the predictive regression is zero. Our findings indicate that all five variables have a strong predictive ability for cryptocurrencies' tail risk connectedness because the null hypothesis of a zero-slope coefficient can be rejected at conventional significance levels in all five univariate regressions. These results confirm the relative importance of investor sentiment and economic conditions in the connectedness of cryptocurrency tail risks.

Out-of-sample prediction

Our last stage of the analysis consists of the out-of-sample forecast performance of the predictors in Eq. (10) compared with a random-walk-with-drift benchmark model, $AR(1)$: $\mathrm{TCI}_t = \beta_0 + \delta \mathrm{TCI}_{t-1} + \varepsilon_{t-1}$. To conduct out-of-sample forecasting, we followed Clark and West (2007) and divided our full sample into an in-sample period spanning from September 11, 2017, to May 30, 2021, and an out-of-sample period from June 1, 2021, to September 30, 2022. Our out-of-sample period, therefore, covers roughly 25% of the entire sample period. We investigate out-of-sample forecasting performance over the forecasting horizons $h \in \{10, 20, 30\}$ days ahead using a recursive window technique. The forecasting performance was evaluated using the mean square forecast error (MSFE)-adjusted statistics from Clark and West (2007). The null hypothesis of the MSFE-adjusted statistics is that the model has no predictability and that the model containing information on investor sentiment/economic conditions does not improve the connectedness of the cryptocurrencies' tail risks.

The results of the MSFE-adjusted statistics in Table 9 confirm the improved predictability of the model containing information on FGCI, ADS, GPR, and TEU conditions at 10, 20, and 30-day horizons with a p-value of 1%. Information on EPU improves the model's forecasting ability at the 5% risk level for all time horizons, whereas, at the 1% risk level, the model's forecasting ability improves at 10 and 20 days. Hence, both the in-sample and out-of-sample findings lead us to conclude that the information contained in investor sentiment and economics includes predictive content about the connectedness of cryptocurrencies in a constant manner. The positive sign of the predictors indicates

Table 9 Out-of-sample prediction (MSFE-adj.)

Forecast	Predictor				
	FGCI	ADS	GPR	EPU	TEU
Panel A: tail risk (CAViaR) at 1%					
Forecast					
h = 10	0.1971***	0.8889***	0.1621***	0.6289***	0.2760***
	[8.8853)	[5.7752]	[4.1803]	[6.9505]	[8.7620]
h = 20	0.2148***	0.8841***	0.1685***	0.6854***	0.2600***
	[9.1126]	[5.7325]	[4.0396]	[6.9834]	[8.6931]
h = 30	0.2088***	0.8709***	0.1652***	0.6541	0. 5216***
	[8.9583]	[5.6825]	[4.0873]	[6.5655]	[8.5269]
Panel B: tail risk (CAViaR) at 5%					
Forecast					
h = 10	0.2143***	0.8969***	0.1325***	0.6313***	0.2319***
	[6.0440]	[6.0440]	[7.1294]	[7.2365]	[6.1240]
h = 20	0.2334***	0.8910***	0.1345***	0.6372***	0.2450***
	[6.0101]	[6.3490]	[7.2534]	[7.2710]	[6.5466]
h = 30	0.2258***	0.8752***	0.1220***	0.6313***	0.2347***
	[5.9808]	[5.0911]	[7.4911]	[7.3861]	[6.6054]

The table presents the Clark and West (2007) mean square forecast error (MSFE)-adjusted statistic comparing the out-of-sample predictions. The in-sample period is taken between 11/10/2017 and 5/30/2021, while the rest is considered as an out-of-sample evaluation forecast period. The results are reported for the forecast horizons ∈ {10, 20, 30}. The null hypothesis of the Clark and West (2007) test is that the model has no predictability; the model containing information on investor sentiment/economic condition does not improve the predictions. Values reported in square brackets are the t-statistics. According to Clark and West (2007), if the t-statistic is larger than + 1.282 (for a one-sided 0.10 test) or + 1.645 (for a one-sided 0.05 test), then the null hypothesis should be rejected. The asymptotic critical values; *** denotes statistic significant at the 1% level (see Clark & West, 2007)

that higher uncertainty (risk) is linked to trading behavior expected to push cryptos in the same direction and is consistent with financial contagion effects.

Additional results

The empirical findings of the Granger causality test and the in-sample and out-of-sample forecasts indicate that the information contained in investor sentiment, economic conditions, and uncertainty includes significant predictive content about the tail risk connectedness of cryptocurrencies. While the abovementioned methods capture the response of one variable to another instantaneously (i.e., at a given point in time), they are silent on the time–horizon relationship, and hence, our results may be subject to some limitations.[12] To validate our results across different time horizons, we employed two novel methods: the cross-quantilogram (CQ) method of Han et al. (2016) and the quantile cross-spectral dependence (QS) approach of Baruník and Kley (2019). The CQ allows us to test the spillover effect between variables across different quantiles. Unlike other methods that focus solely on the direction of the relationship, the CQ method allows for a simultaneous assessment of the link between two variables in terms of their duration and direction by considering long lags (Sohag et al. 2022,2023a, b; Husain et al. 2022). QS is valuable because it captures the interdependence between variables at different

[12] This point has been brought to our attention, thankfully, by one of the referees.

time frequencies and quantiles. The following section provides a brief overview of the proposed method.[13]

Cross-quantilogram (CQ) method As in Han et al. (2016), let there be a set of $\boldsymbol{X}_t = \left(x_{t,j1}, x_{t,j2}\right)$ that are two strictly stationary series, cross-quantilogram is defined as the cross-correlation of the quantile-exceedance processes $\left\{x_{1t-k} \leq q_{1t-k}(\tau_1)\right\}$ and $\left\{x_{2t-k} \leq q_{2t-k}(\tau_2)\right\}$ where $q_{it-k}(\tau_i)$ is the conditional $\tau_i -$ quantile of x_{it} for $\tau_i \in (0,1)$, for $i = 1, 2$, and $k = 0, \mp 1, \mp 2, \ldots$ represents the lag length that is able to capture the cross-quantile dependence between the variables across various time horizons, thereby quantifying the strength and duration of dependency. The cross-correlation of the various quantile-hit processes is then described as

$$\rho_\tau(k) = \frac{E\left[\psi_{\tau 1}(x_{1t} - q_{1t}(\tau_1))\psi_{\tau 2}\left(x_{2t-k} - q_{2t-k}(\tau_2)\right)\right]}{\sqrt{E\left[\psi_{\tau 1}^2(x_{1t} - q_{1t}(\tau_1))\right]}\sqrt{\psi_{\tau 2}^2\left(x_{2t-k} - q_{2t}(\tau_2)\right)}} \tag{11}$$

where $\psi_\tau(x_{1t}) \equiv 1[y_{1t} \leq q_{1t}(\tau_i)]\text{-}\tau_i$ represents the quantile-hit process.$\widehat{\rho_\tau}(k) \in [-1, 1]$ with $\widehat{\rho_\tau}(k) = 0$ indicates the absence of any cross-dependence between the variables.

Han et al. (2016) recommend using a quantile version of the Box-Ljung statistics to test for directional predictability from one time series to another over a set of quantiles $\widehat{Q}_\tau(K)$, as follows

$$\widehat{Q}_\tau(K) \equiv \frac{T(T+2)\sum_{k=1}^{p}\widehat{\sigma}_\tau^2}{T-k} \tag{12}$$

The cross-quantilograms between the tail risk connectedness at 5% and each predictor are displayed in Fig. 13.[14] We report the cross-quantilograms of lag k = 1, 2, …, 60 over the lower (α = 0.05), middle (α = 0.5), and extreme upper (α = 0.95) quantiles.

The results generally show that the predictor variables at the lower quantile (α = 0.05) are positively and statistically significantly correlated with cryptocurrencies' tail risk connectedness at most lags, except for ADS, where dependence is mostly negative. In the middle quantile (α = 0.50), we again observed that the CQs were mostly positive and significant in both the short and long runs, suggesting that the predictability from FGCI, GPR, and TEU to the connectedness of cryptocurrencies is positive during normal states. For ADS, the CQs were negative and statistically significant from 20 days to 50. Furthermore, we found substantial positive directional prediction at the longest lags when the predictor variables were at the extreme upper quantiles (α = 0.95). The Box-Ljung (portmanteau) statistics displayed in Fig. 14 provide additional confirmation of the significant cross-quantilogram correlation.

Quantile cross-spectral method Similar to the CQ approach, let $\boldsymbol{X}t$ to be two stationary time-series, with components $\boldsymbol{X}_t = \left(x_{t,j1}, x_{t,j2}\right)$, the quantile coherency between these two processes ($\mathfrak{R}^{j_1,j_2}$) can be written as

[13] Recently, several studies applied the cross-quantilogram method (e.g., Sohag et al. 2023a; Maghyereh and Abdoh 2020a, b, 2021a, b, c, 2022b; Khalfaoui et al. 2021).

[14] We also estimate the cross-quantilograms between the tail risk connectedness at 1% and each predictor (to save on space, the results are not reported but are available from the authors upon request) and find similar results.

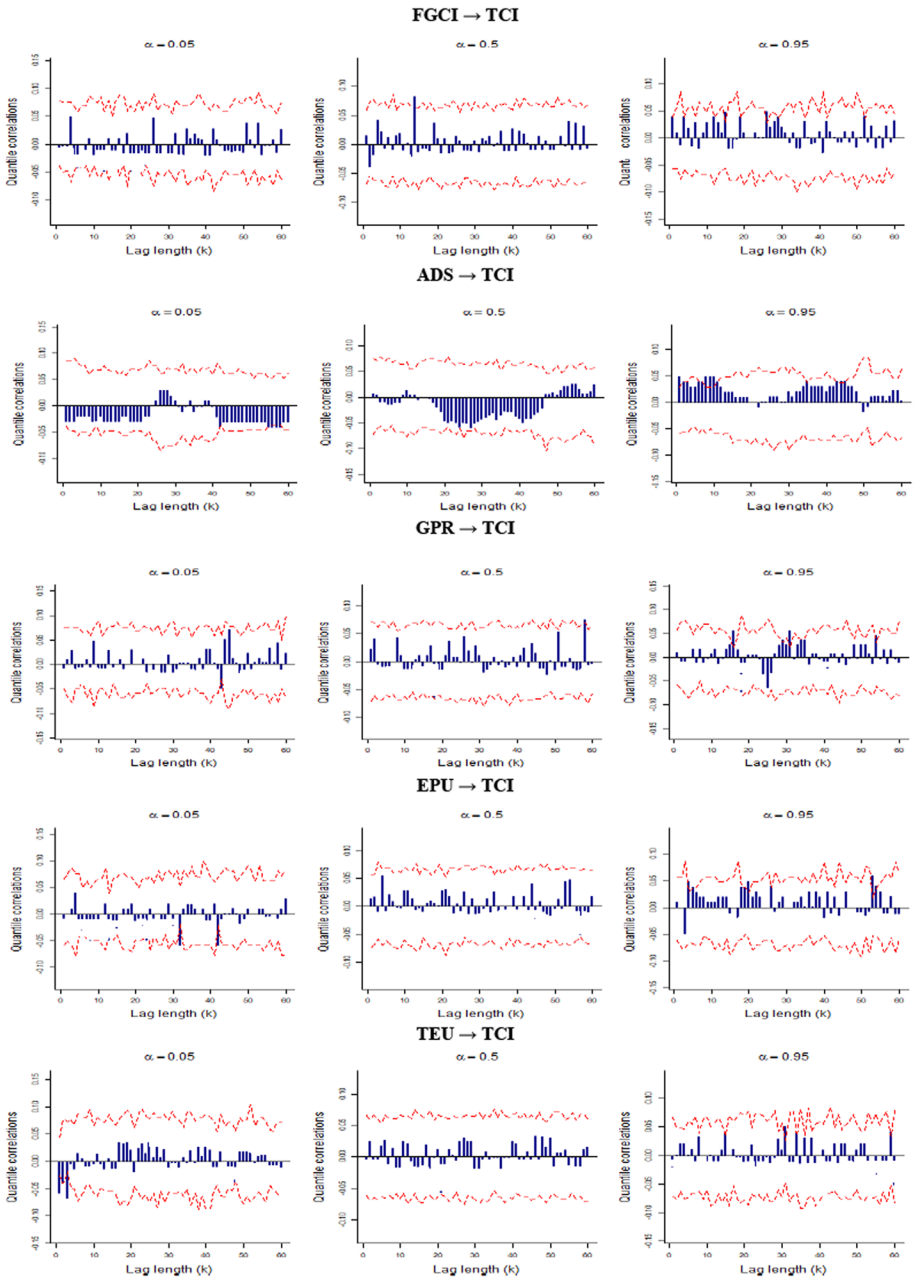

Fig. 13 Cross-quantilograms correlation. *Note*: The figure plots the directional predictability from each predictor variable to total tail risk connectedness index estimated at 5% CAViaRs. The graph depicts the directional predictability at lag k = 1, 2, …, 60 over the lower quantile (α = 0.05), middle (α = 0.5), and extreme upper (α = 0.95) quantiles. The 95% bootstrap confidence intervals are indicated by the red dotted lines

$$\Re^{j_1,j_2}(\omega;\tau_1,\tau_2) := \frac{f^{j_1,j_2}(\omega;\tau_1,\tau_2)}{\left(f^{j_1,j_1}(\omega;\tau_1,\tau_1)f^{j_2,j_2}(\omega;\tau_2,\tau_2)\right)^{1/2}} \tag{13}$$

where f^{j_1,j_2}, f^{j_1,j_1} and f^{j_2,j_2} are the quantile cross-spectral density and the quantile spectral densities of variables, $-\pi < \omega < \pi$ and $(\tau_1,\tau_2) \in [0,1]$, obtained from the Fourier

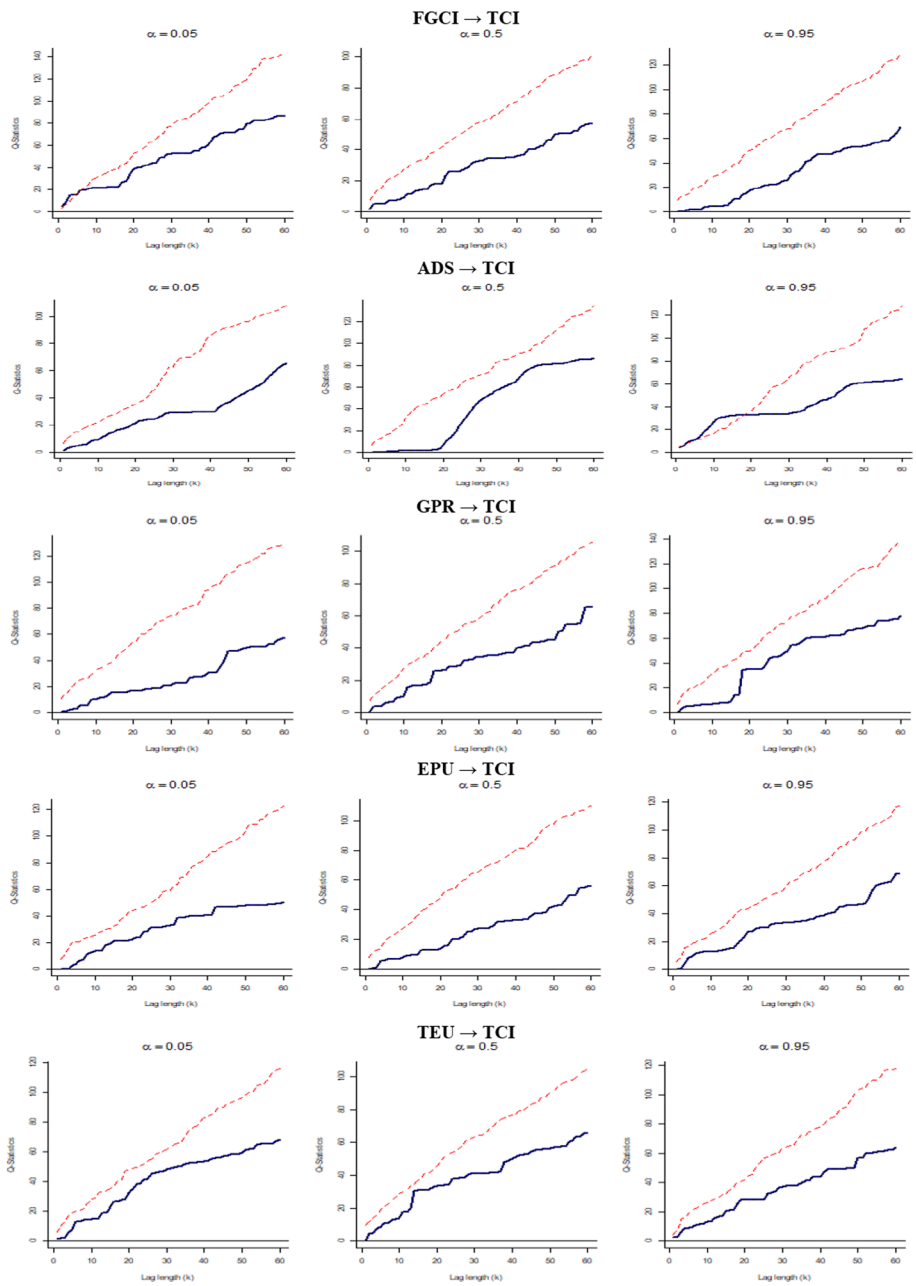

Fig. 14 Box–Ljung test statistic. *Note*: The figure plots Box–Ljung test statistic between each predictor variable to total tail risk connectedness index estimated at 5% CAViaRs The 95% bootstrap confidence intervals are indicated by the red dotted lines

transform of the matrix of quantile cross-covariance kernels $\Gamma(\tau_1, \tau_2) := \left(f(\omega; \tau_1, \tau_2)\right)_{j_1,j_2}$, where

$$\gamma_k^{j_1,j_2} := Cov\left(I\left\{X_{t+k,j_1,} \leq q_{j_1(\tau_1)}\right\}, I\left\{X_{t+k,j_2,} \leq q_{j_2(\tau_2)}\right\}\right) \tag{14}$$

for $j_1, j_2 \in \left\{1, \ldots, d\right\}$, $k \in \digamma, \tau_1, \tau_2 \in [0, 1]$, and I{A} is the indicator function of event A. The frequency domain matrix of quantile cross-spectral density kernels is $f(\omega; \tau_1, \tau_2)$:

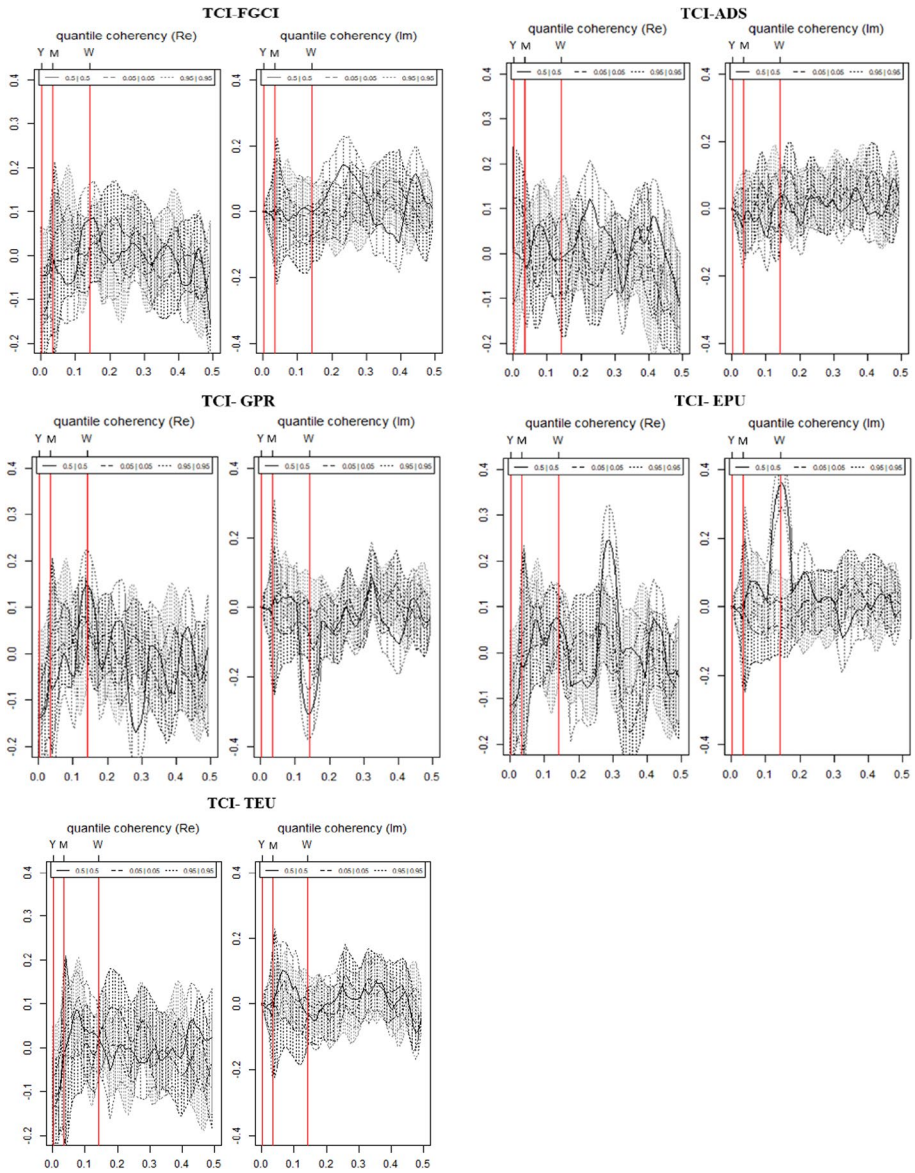

Fig. 15 Quantile coherency. *Notes*: Plot of the real (left) and imaginary (right) parts of the quantile coherency at 0.05, 0.5, and 0.95 quantiles with 95% confidence intervals. W, M, and Y denotes weekly, monthly, and yearly periods

$=\left(f(\omega;\tau_1,\tau_2)\right)_{j_1,j_2}$. According to Barunik and Kley (2019), quantile coherency is estimated as follows

$$\widehat{\Re}_{n,R}^{j_1,j_2}(\omega;\tau_1,\tau_2) := \frac{\widehat{G}_{n,R}^{j_1,j_2}(\omega;\tau_1,\tau_2)}{\left(\widehat{G}_{n,R}^{j_1,j_1}(\omega;\tau_1,\tau_1)\widehat{G}_{n,R}^{j_2,j_2}(\omega;\tau_2,\tau_2)\right)^{\frac{1}{2}}} \tag{15}$$

where $\widehat{G}_{n,R}^{j_1,j_2}$ are the smoothed quantile cross-periodograms, $I_{n,R}^{j_1,j_2}$ is the rank-based copula cross-periodogram matrices (CCR-periodograms), and W_n is a sequence of weight functions.

The coherence between the tail risk connectedness at 5% and each predictor indicated is reported in Fig. 15.[15] The plots show the real (left) and imaginary (right) parts of the quantile coherency for the lower (0.05|0.05), middle (0.5|0.5), and higher quantiles (0.95|0.95). The daily cycles over the intervals are shown on the horizontal axis, whereas the vertical axis measures the magnitude of the co-dependence between the two variables. The upper label (W, M, Y) of the horizontal axis shows the time frequencies corresponding to the weekly (short run), monthly (medium run), and yearly (long run) periods. These time frequencies translate to $\omega \in 2\pi\{1/7, 1/30, 1/365\}$.

Figures reveal a positive coherency between the tail risk connectedness of cryptocurrencies and the FGCI, ADS, GPR, EPU, and TEU conditions across all quantile ranges between − 0.1 and 0.2 in the short-run dynamics (i.e., at weekly cycles). However, this quantile coherency became stronger during lower quantiles (i.e., 0.05|0.05 quantiles) and extreme conditions (i.e., 0.95|0.95 quantiles) for (i.e., at monthly and yearly cycles). In other words, these results reveal significant upper quantiles and long-run dependence, whereas the real coherency is between − 0.2 and 0.6 during the middle quantiles of the joint distribution and between − 0.2 and 0.2 during the upper quantiles of the joint distribution quantiles. Overall, the findings indicate the predictive abilities of the FGCI, ADS, GPR, EPU, and TEU conditions across all time horizons.

Conclusion

Motivated by cryptocurrencies' increasing importance and popularity in the financial arena, this study examines tail connectedness among cryptocurrencies and their underlying factors. The main results indicate an increasing level of tail connectedness during turbulent periods. ETC is the main influencer among cryptocurrencies despite having lower capitalization than BTC. Simultaneously, an increase in the dynamics of BNB, XRP, and ADA is expected in 2022. Finally, the highest pairwise connectedness is between ETC and BTC.

Our analysis is important to both investors and portfolio managers. In essence, a cryptocurrency portfolio comprising the most popular cryptocurrencies involves a high level of dependency, which means investors should exercise extreme caution when positioning highly interconnected cryptocurrencies such as BTC and ETC. In a possible collapse, these cryptocurrencies would represent a substantial portion of total cryptocurrency capitalization. This is particularly important given that cryptocurrencies present heavier tail distributions, implying unusually high levels of tail risk.

Policymakers and regulators should also be particularly cautious during extraordinary periods, as cryptocurrency selloffs due to herding behavior and panic can lead to severe consequences and bankruptcy. Innovations from ETC and XRP (despite their lower extent) appeared to have the largest footprints in the system. Hence, policymakers can counter ETC innovations before they become widespread and cause market turbulence.

Finally, in predicting the TCI level among cryptocurrencies, the MSFE-adjusted statistics confirmed the improved predictability of the model containing information on the FGCI, ADS, GPR, EPU, and TEU conditions at multiple investment horizons with

[15] We also estimate the coherency between the tail risk connectedness at 1% and each predictor (to save on space, the results are not reported but are available from the authors upon request) and find similar results.

high significance. This means policymakers can use our metrics to forecast periods with notably high TCI and take the necessary measures to mitigate financial contagion and preserve financial stability. This finding does not comply with the notion of increasing cryptos' efficiency, as Noda (2021) argued. Hence, our study provides new evidence of the inefficiency of cryptocurrencies.

Abbreviations

CAViaR	Conditional autoregressive Value-at-Risk
TVP-VAR	Time-varying parameter vector autoregressive
VaR	Value at risk
COVID-19	Coronavirus disease
DQ	Dynamic quantile
GFEVD	Generalized forecast error variance decompositions
BIC	Bayesian information criterion
TCI	Total connectivity index
BTC	Bitcoin
ETC	Ethereum
USD	Tether
BNB	Binance
ADA	Cardano
NPT	Net pairwise directional connectedness
FGCI	Fear and greed crypto index
ADS	Aruoba-Diebold-Scotti business condition index
GPR	Geopolitical risk index
EPU	Economic policy uncertainty index
TEU	Twitter-based economic uncertainty index
MSFE	Mean square forecast error

Acknowledgements
The authors thank the anonymous reviewers of this manuscript.

Author contributions
AM: Initiated the subject, contributed to the methodologies, collected data, analyzed the data in MATLAP, R and Stata, interpretation and discussion of results, and editing. SZ: Review of literature, and wrote the first manuscript. The author(s) read and approved the final manuscript.

Funding
We did not get any funding for this article.

Availability of data and materials
All data are obtained from Thomson Reuters Datastream database. The models and data analysis are applied through computer software such as MATLAB, R, and Stata. All data and codes will be available from the authors upon request upon request.

Declarations

Competing interests
The authors declare that they have no competing interests.

Received: 16 January 2023 Accepted: 18 December 2023
Published online: 01 March 2024

References

Adrian T, Brunnermeier MK (2016) CoVaR. Am Econ Rev 106(7):1705–1741
Al-Shboul M, Assaf A, Mokni K (2022) When bitcoin lost its position: cryptocurrency uncertainty and the dynamic spillover among cryptocurrencies before and during the COVID-19 pandemic. Int Rev Financ Anal 83:102309
Antonakakis N, Chatziantoniou I, Gabauer D (2020) Refined measures of dynamic connectedness based on time-varying parameter vector autoregressions. J Risk Financ Manag 13(4):84
Beine M, Cosma A, Vermeulen R (2010) The dark side of global integration: increasing tail dependence. J Bank Finance 34(1):184–192
Baker S, Nicholas B, Steven JD (2016) Measuring economic policy uncertainty. Quart J Econ 131(4):1593–1636
Baruník J, Kley T (2019) Quantile coherency: A general measure for dependence between cyclical economic variables. Econ J 22(2):131–152
Borri N (2019) Conditional tail-risk in cryptocurrency markets. J Empir Financ 50:1–19

Bouri E, Azzi G, Dyhrberg AH (2017a) On the return-volatility relationship in the Bitcoin market around the price crash of 2013. Economics 11(1):2
Bouri E, Gabauer D, Gupta R, Tiwari AK (2021a) Volatility connectedness of major cryptocurrencies: the role of investor happiness. J Behav Exp Financ 30:100463
Bouri E, Gupta R, Tiwari AK, Roubaud D (2017b) Does Bitcoin hedge global uncertainty? Evidence from wavelet-based quantile-in-quantile regressions. Financ Res Lett 23:87–95
Bouri E, Saeed T, Vo XV, Roubaud D (2021b) Quantile connectedness in the cryptocurrency market. J Int Finan Mark Inst Money 71:101302
Bouri E, Vo XV, Saeed T (2021c) Return equicorrelation in the cryptocurrency market: analysis and determinants. Financ Res Lett 38:101497
Caldara D, Iacoviello M (2022) Measuring geopolitical risk. Amer. Econ Rev 112(4):1194–1225
Canh NP, Wongchoti U, Thanh SD, Thong NT (2019) Systematic risk in cryptocurrency market: evidence from DCC-MGARCH model. Financ Res Lett 29:90–100
Chatziantoniou I, Gabauer D, de Gracia FP (2022) Tail risk connectedness in the refined petroleum market: a first look at the impact of the COVID-19 pandemic. Energy Economics 111:106051
Clark TD, West KD (2007) Approximately normal tests for equal predictive accuracy in nested models. J Econ 138(1):291–311
Corbet S, Meegan A, Larkin C, Lucey B, Yarovaya L (2018) Exploring the dynamic relationships between cryptocurrencies and other financial assets. Econ Lett 165:28–34
Corsetti G, Pericoli M, Sbracia M (2005) 'Some contagion, some interdependence': more pitfalls in tests of financial contagion. J Int Money Financ 24(8):1177–1199
Cui J, Maghyereh A (2022) Time–frequency co-movement and risk connectedness among cryptocurrencies: new evidence from the higher-order moments before and during the COVID-19 pandemic. Financ Innov 8(1):1–56
Cui J, Maghyereh A (2023a) Time-frequency dependence and connectedness among global oil markets: fresh evidence from higher-order moment perspective. J Commod Mark 30:100323
Cui J, Maghyereh A (2023b) Higher-order moment risk connectedness and optimal investment strategies between international oil and commodity futures markets: insights from the COVID-19 pandemic and Russia-Ukraine conflict. Int Rev Financ Anal 86:102520
Danielsson J, de Vries CG (2000) Value-at-Risk and extreme returns. Annales D'economie Et De Statistique 60:236–269
Diebold FX, Yilmaz K (2009) Measuring financial asset return and volatility spillovers, with application to global equity markets. Econ J 119(534):158–171
Diebold FX, Yilmaz K (2012) Better to give than to receive: predictive directional measurement of volatility spillovers. Int J Forecast 28(1):57–66
Diebold FX, Yılmaz K (2014) On the network topology of variance decompositions: measuring the connectedness of financial firms. J Econom 182(1):119–134
Engle RF, Ito T, Lin WL (1990) Meteor showers or heat waves? Heteroskedastic intra-daily volatility in the foreign exchange market. Econometrica 58:525–542
Engle RF, Manganelli S (2004a) CAViaR: conditional autoregressive value at risk by regression quantiles. J Bus Econ Stat 22(4):367–381
Fang F, Ventre C, Basios M, Kanthan L, Martinez-Rego D, Wu F, Li L (2022) Cryptocurrency trading: a comprehensive survey. Financ Innov 8(1):1–59
Ferreira P, Kristoufek L, Pereira EJAL (2020) DCCA and DMCA correlations of cryptocurrency markets. Physica A 545:123803
Forbes KJ, Rigobon R (2002) No contagion, only interdependence: measuring stock market comovements. J Financ 57(5):2223–2261
Geuder J, Kinateder H, Wagner NF (2019) Cryptocurrencies as financial bubbles: the case of Bitcoin. Finance Res Lett 31:179–184
Gillaizeau M, Jayasekera R, Maaitah A, Mishra T, Parhi M, Volokitina E (2019) Giver and the receiver: understanding spillover effects and predictive power in cross-market Bitcoin prices. Int Rev Financ Anal 63:86–104
Han H, Linton O, Oka T, Whang Y (2016) The cross-quantilogram: measuring quantile dependence and testing directional predictability between time series. J Econom 193:251–270
Hu Y, Valera HGA, Oxley L (2019) Market efficiency of the top market-cap cryptocurrencies: further evidence from a panel framework. Financ Res Lett 31:138–145
Husain S, Sohag K, Wu Y (2022) The response of green energy and technology investment to climate policy uncertainty: an application of twin transitions strategy. Technol Soc 71:102132
Ji Q, Bouri E, Lau CKM, Roubaud D (2019) Dynamic connectedness and integration in cryptocurrency markets. Int Rev Financ Anal 63:257–272
Karim S, Lucey BM, Naeem MA, Uddin GS (2022) Examining the interrelatedness of NFTs, DeFi tokens and cryptocurrencies. Financ Res Lett 47:102696
Karolyi GA, Stulz RM (1996) Why do markets move together? An investigation of US-Japan stock return comovements. J Financ 51(3):951–986
Katsiampa P (2017) Volatility estimation for Bitcoin: a comparison of GARCH models. Econ Lett 158:3–6
Katsiampa P, Corbet S, Lucey B (2019) High frequency volatility co-movements in cryptocurrency markets. J Int Finan Mark Inst Money 62:35–52
Khalfaoui R, Tiwari AK, Kablan S, Hammoudeh S (2021) Interdependence and lead-lag relationships between the oil price and metal markets: fresh insights from the wavelet and quantile coherency approaches. Energy Econ 101:105421
Kim SJ, Moshirian F, Wu E (2005) Dynamic stock market integration driven by the European Monetary Union: an empirical analysis. J Bank Finance 29(10):2475–2502
Koenker R, Hallock KF (2001) Quantile Regression. J Econ Perspect 15(4):143–156
Koop G, Pesaran MH, Potter SM (1996) Impulse response analysis in nonlinear multivariate models. J Econom 74(1):119–147

Koutmos D (2018) Return and volatility spillovers among cryptocurrencies. Econ Lett 173:122–127
Kumar AS, Anandarao S (2019) Volatility spillover in crypto-currency markets: some evidences from GARCH and wavelet analysis. Physica A 524:448–458
Kumar A, Iqbal N, Mitra SK, Kristoufek L, Bouri E (2022) Connectedness among major cryptocurrencies in standard times and during the COVID-19 outbreak. J Int Finan Mark Inst Money 77:101523
Luu Duc Huynh T (2019) Spillover risks on cryptocurrency markets: a look from VAR-SVAR granger causality and student's copulas. J Risk Financ Manag 12(2):52
Maghyereh A, Abdoh H (2020a) The tail dependence structure between investor sentiment and commodity markets. Resour Policy 68:101789
Maghyereh A, Abdoh H (2020b) Tail dependence between Bitcoin and financial assets: evidence from a quantile cross-spectral approach. Int Rev Financ Anal 71:101545
Maghyereh A, Abdoh H (2021a) Time–frequency quantile dependence between Bitcoin and global equity markets. N Am J Econ Finance 56:101355
Maghyereh A, Abdoh H (2021b) Tail dependence between gold and Islamic securities. Financ Res Lett 38:101503
Maghyereh A, Abdoh H (2021c) The impact of extreme structural oil-price shocks on clean energy and oil stocks. Energy 225:120209
Maghyereh A, Abdoh H (2022a) COVID-19 and the volatility interlinkage between bitcoin and financial assets. Empir Econ 63:2875–2901
Maghyereh A, Abdoh H (2022b) Extreme dependence between structural oil shocks and stock markets in GCC countries. Resour Policy 76:102626
Maghyereh A, Yamani E (2022) Does bank income diversification affect systemic risk: new evidence from dual banking systems. Financ Res Lett 47:102814
Maghyereh A, Al-Shboul M (2023) Have the extraordinary circumstances of the COVID-19 outbreak and the Russian-Ukrainian conflict impacted the efficiency of cryptocurrencies? Financ Innov, Forthcoming.
Maghyereh A, Abdoh H, Awartani B (2022) Have returns and volatilities for financial assets responded to implied volatility during the COVID-19 pandemic? J Commod Mark 26:100194
Morana C, Beltratti A (2008) Comovements in international stock markets. J Int Finan Markets Inst Money 18(1):31–45
Nakamoto S (2008) Bitcoin: a peer-to-peer electronic cash system. Available at SSRN: https://ssrn.com/abstract=3440802 or https://doi.org/10.2139/ssrn.3440802
Noda A (2016) A test of the adaptive market hypothesis using a time-varying AR model in Japan. Financ Res Lett 17:66–71
Noda A (2021) On the evolution of cryptocurrency market efficiency. Appl Econ Lett 28(6):433–439
Omane-Adjepong M, Alagidede IP (2019) Multiresolution analysis and spillovers of major cryptocurrency markets. Res Int Bus Financ 49:191–206
De Pace P, Rao J (2023) Comovement and instability in cryptocurrency markets. Int Rev Econ Financ 83:173–200
Patton AJ, Ziegel JF, Chen R (2019) Dynamic semiparametric models for expected shortfall (and value-at-risk). J Econom 211(2):388–413
Pesaran HH, Shin Y (1998) Generalized impulse response analysis in linear multivariate models. Econ Lett 58(1):17–29
Salisu AA, Olaniran A, Tchankam JP (2022) Oil tail risk and the tail risk of the US Dollar exchange rates. Energy Econ 109:105960
Salisu AA, Omoke PC, Sikiru AA (2023) Geopolitical risk and global financial cycle: some forecasting experiments. J Forecast 42(1):3–16
Sebastião H, Godinho P (2021) Forecasting and trading cryptocurrencies with machine learning under changing market conditions. Financ Innov 7(1):1–30
Shi S, Hurn S, Phillips PCB (2020) Causal change detection in possibly integrated systems: Revisiting the money–income relationship. J Financ Econ 18(1):158–180
Sohag K, Hammoudeh S, Elsayed AH, Mariev O, Safonova Y (2022) Do geopolitical events transmit opportunity or threat to green markets? Decomposed measures of geopolitical risks. Energy Econ 111:106068
Sohag K, Hassan MK, Bakhteyev S, Mariev O (2023a) Do green and dirty investments hedge each other? Energy Economics 120:106573
Sohag K, Shams SR, Gainetdinova A, Nappo F (2023b) Frequency connectedness and cross-quantile dependence among medicare, medicine prices and health-tech equity. Technovation 120:102483
Sohag K, Ullah M (2022) Response of BTC Market to social media sentiment: application of cross-quantilogram with bootstrap. In: Digitalization and the future of financial services: innovation and impact of digital finance, pp 103–119. Springer, Cham
Tran V, Leirvik T (2019) A simple but powerful measure of market efficiency. Financ Res Lett 29:141–151
Tran V, Leirvik T (2020) Efficiency in the markets of crypto-currencies. Financ Res Lett 35:101382
Urquhart A, Zhang H (2019) Is Bitcoin a hedge or safe haven for currencies? An intraday analysis. Int Rev Financ Anal 63:49–57
Wang H, Wang X, Yin S, Ji H (2022) The asymmetric contagion effect between stock market and cryptocurrency market. Financ Res Lett 46:102345
Wang C, Gerlach R, Chen Q (2018) A semi-parametric realized joint value-at-risk and expected shortfall regression framework. http://arxiv.org/abs/1807.02422
Westerlund J, Narayan PK (2012) Does the choice of estimator matter when forecasting returns? J Bank Finance 36(9):2632–2640
Westerlund J, Narayan PK (2015) Testing for predictability in conditionally heteroskedastic stock returns. J Financ Economet 13(2):342–375
White H, Kim TH, Manganelli S (2015) VAR for VaR: measuring tail dependence using multivariate regression quantiles. J Econom 187(1):169–188
Xu M, Chen X, Kou G (2019) A systematic review of blockchain. Financ Innov 5(1):1–14
Xu Q, Zhang Y, Zhang Z (2021) Tail-risk spillovers in cryptocurrency markets. Financ Res Lett 38:101453

Yermack D (2017) Corporate governance and blockchains. Rev Finance 21(1):7–31
Yi S, Xu Z, Wang GJ (2018) Volatility connectedness in the cryptocurrency market: is bitcoin a dominant cryptocurrency? Int Rev Financ Anal 60:98–114

Publisher's Note